Acta Pharmaceutica Sinica B 2026;16(4):1943−1970

Chinese Pharmaceutical Association
Institute of Materia Medica, Chinese Academy of Medical Sciences

Acta Pharmaceutica Sinica B

www.elsevier.com/locate/apsb
www.sciencedirect.com

REVIEW

Deciphering the biological fate of mRNA-LNP-based biologics: A perspective from tissue to intracellular distribution

Xin Xu[a], Lili Cui[b], Yong Zhang[c,*], Jingkai Gu[a,d,*]

[a]*Research Center for Drug Metabolism, School of Life Sciences, Jilin University, Changchun 130012, China*
[b]*Beijing Research Center, CSPC Pharmaceutical Group Limited, Beijing 102629, China*
[c]*National Engineering Laboratory for AIDS Vaccine, School of Life Sciences, Jilin University, Changchun 130012, China*
[d]*State Key Laboratory of Supramolecular Structure and Materials, Center for Supramolecular Chemical Biology, College of Chemistry, Jilin University, Changchun 130012, China*

Received 15 May 2025; received in revised form 26 July 2025; accepted 21 August 2025

KEY WORDS

mRNA-LNP;
Biodistribution;
Cellular uptake;
Endosomal escape;
Pharmacokinetics;
Analytical methodology;
Ionizable lipids;
Protein expression

Abstract The remarkable clinical success of mRNA-lipid nanoparticle (mRNA-LNP) vaccines, particularly evidenced by their pandemic-era impact and subsequent 2023 Nobel Prize recognition, has intensified global efforts to expand their application toward therapeutic biologics. Despite showing strong preventive effects, there are still fundamental knowledge gaps in comprehensively defining the hierarchical biological trajectory of mRNA-LNP formulations, which spans from initial systemic exposure, tissue-specific biodistribution, and intracellular delivery to ultimate protein expression dynamics. These unresolved mechanistic questions pose significant constraints on the rational design of next-generation mRNA-LNP therapeutics, which face increased demands for precision dosing, therapeutic efficacy optimization, and enhanced safety profiles. This review discusses the *in vivo* fate of mRNA-LNP, focusing specifically on blood/tissue/cellular distribution and kinetics/exposure profiles of both intact mRNA-LNP and dissociated components post-administration. It discusses key factors influencing the distribution of expressed protein and summarizes the corresponding research toolkits along with their advantages and disadvantages. Additionally, it compiles strategies to enhance delivery efficacy, tissue tropism, and safety profiles of mRNA-LNP. We anticipate a better understanding of the biological processes and dynamic pattern of mRNA-LNP, which will accelerate the development of next-generation mRNA biologics with predictable safety and delivery efficiency.

This article is part of special issue entitled: Hot Topic Revs in Drug Delivery (II) published in Acta Pharmaceutica Sinica B.
*Corresponding authors.
E-mail addresses: zhypharm@jlu.edu.cn (Yong Zhang), gujk@jlu.edu.cn (Jingkai Gu).
Peer review under the responsibility of Chinese Pharmaceutical Association and Institute of Materia Medica, Chinese Academy of Medical Sciences.

https://doi.org/10.1016/j.apsb.2025.11.023
2211-3835 © 2025 The Authors. Published by Elsevier B.V. on behalf of Chinese Pharmaceutical Association and Institute of Materia Medica, Chinese Academy of Medical Sciences. This is an open access article under the CC BY-NC-ND license (http://creativecommons.org/licenses/by-nc-nd/4.0/).

© 2025 The Authors. Published by Elsevier B.V. on behalf of Chinese Pharmaceutical Association and Institute of Materia Medica, Chinese Academy of Medical Sciences. This is an open access article under the CC BY-NC-ND license (http://creativecommons.org/licenses/by-nc-nd/4.0/).

1. Introduction

During the global COVID-19 pandemic, two lipid nanoparticle-based messenger RNA (mRNA-LNP) vaccines, Comirnaty® (BNT162b2, BioNTech/Pfizer) and Spikevax® (mRNA-1273, Moderna), received emergency use authorization from the US Food and Drug Administration (FDA) at an unprecedented speed and have made substantial contributions to global epidemic prevention and control. Their success primarily stems from two revolutionary technologies: 1) the nucleotide-modified mRNA enabling evasion of the body's innate immune surveillance; 2) the ionizable lipid nanoparticle-based cytoplasmic delivery systems. Beyond pandemic applications, the mRNA-LNP outperforms conventional vaccines in antigen design flexibility and scalable manufacturing, which are critical advantages for combating emerging pathogens. To date, over 200 mRNA-LNP vaccines have entered clinical trials (based on the data of clinicaltrials.gov), only a few approved for COVID-19 (Table 1[1-21]). The clinical validation of this platform has catalyzed its expansion into three frontiers: the preventive vaccines against diverse pathogens, personalized cancer neoantigen therapies and gene editing (Fig. 1). In May 2024, the FDA approved mRNA-1345 (MRESVIA®), the first mRNA-LNP vaccine against lower respiratory tract disease caused by respiratory syncytial virus (RSV) in adults ≥60 years old (Table 1)[22]. Simultaneously, the individualized neoantigen vaccine mRNA-4157 (V940) combined with pembrolizumab showed a 49% reduction in recurrence or death risk and a 62% reduction in distant metastasis or death risk in Phase 2b melanoma trials, demonstrating significantly improved survival benefits[23]. Additionally, in a Phase 1 clinical trial, NTLA-2001—a first-in-human *in vivo* gene therapy comprising mRNA-LNP that encapsulates both guide RNA (gRNA) and optimized Cas9-encoding mRNA—achieved a reduction in serum transthyretin of 47%−56% in the low-dose group and 80%−96% in the high-dose group, with no serious adverse events reported[24]. In another Phase 1 clinical trial, VERVE-101—an LNP-based therapy delivering both mRNA for an adenine base editor and a gRNA—silenced the *PCSK9* gene *via* A-to-G base editing with dose-dependent effects. At the high dose of 0.6 mg/kg, it achieved a 55% reduction in blood low-density lipoprotein cholesterol, with effects persisting for up to 180 days[25,26].

Despite the remarkable therapeutic potential of mRNA-LNP technology in addressing unmet clinical needs, critical knowledge gaps persist in understanding its *in vivo* fate: particularly those aspects closely linked to its efficacy and safety profile. These limitations significantly impede the development of next-generation mRNA-LNP-based therapeutic agents, including protein replacement therapy, gene editing, and *in vivo* chimeric antigen receptor T-cell immunotherapy, which require more stringent standards for dosing, delivery, sustained protein expression, and safety. It is well established that mRNA-LNP vaccines can effectively activate innate and adaptive immune systems to elicit robust protective humoral and cellular immune responses, even when administered locally (*e.g.*, intramuscular or subcutaneous route) at low doses with a delivery efficiency of less than 1%[27,28]. In contrast, mRNA-LNP-based protein replacement therapy typically requires precise tissue/cell-specific targeting and sustained high-level protein expression, which may be more than 1000 times the expression of vaccine protein[29]. Increasing the dosage of existing mRNA-LNP formulations to achieve elevated target protein expression is clearly impractical, as current mRNA-LNP vaccines have already demonstrated many adverse effects (*e.g.*, pain, swelling, fever, drowsiness, headache, and so on) with increased incidence rates in clinical trials and real-world applications when compared to conventional vaccines[30-32]. Dose escalation will likely result in heightened adverse effect profiles with increased incidence and severity. Moreover, efficient tissue/cell-specific targeted delivery presents significantly greater challenges, as it necessitates strategic coordination on mRNA-LNP components and physicochemical properties to address multifaceted physiological barriers. These include systemic clearance mediated by metabolic enzymes and the mononuclear phagocyte system, dynamic cellular uptake-exocytosis equilibrium, and endolysosomal trafficking/escape, while concurrently addressing critical delivery issues such as optimization of off-target biodistribution and controlled cytoplasmic mRNA release.

Given these challenges and the high adverse event rates associated with current mRNA-LNP vaccines[33], a critical imperative exists to elucidate the spatiotemporal biodistribution profiles and molecular interactions of intact nanoparticles and their core components within complex biological microenvironments. These insights will be pivotal in guiding the rational design and system-level optimization of mRNA-LNP platforms, facilitating precise tissue-specific targeting, improved delivery efficiency, and optimal desired risk/benefit balance. This review focuses on the current landscape of the *in vivo* fate of mRNA-LNPs, with particular emphasis on their blood/tissue/cellular distribution and kinetics/exposure profiles, along with those of their key components following administration. It further explores the key factors influencing their distribution, critically evaluates current analytical methodologies, and highlights advanced strategies for enhancing delivery efficiency, targeting, and safety. By elucidating the biological processes and systemic dynamics, this review seeks to advance the development of next-generation mRNA-LNP biologics with refined safety profiles and superior delivery.

2. Composition, structure, and preparation techniques of mRNA-LNPs

mRNA-LNPs are typically composed of mRNA and four lipid components: ionizable lipid (ILs), PEG-lipid, DSPC (1,2-distearoyl-*sn*-glycero-3-phosphocholine), and cholesterol. Each fulfilling distinct functional roles essential for nanoparticle integrity and mRNA delivery, as detailed in Fig. 2. Structurally, mRNA-LNPs are spherical vesicles with an optimal particle size range of 50−200 nm. The precise internal microstructure of these mRNA-LNPs is influenced by various factors, including formulation components and manufacturing processes[34,35]. It is generally accepted that currently two marketed mRNA-LNP vaccines predominantly possess a nanostructured core−shell architecture (Fig. 2)[36-38].

mRNA-LNPs are typically formed by mixing ethanolic lipid solutions with mRNA dissolved in an acidic aqueous buffer. Thin-

Table 1 Representative mRNA-LNP-based biologics.

Product Name	Antigen/protein	Disease	LNP composition	Administration route	Dose	Trial Number	Phase	Status	Sponsor	Ref.
Infectious disease										
BNT162b2	SARS-CoV-2 full-length spike protein	COVID-19	ALC0315, cholesterol, DSPC, ALC0159 = 46.3:42.7:9.4:1.6	Intramuscular injection	30 μg	NCT04368728	Approved	Completed	BioNTech SE	1
mRNA-1273	Prefusion stabilized full-length spike protein	COVID-19	SM102, cholesterol, DSPC, DMG-PEG 2000 = 50:38.5:10:1.5	Intramuscular injection	100 μg	NCT04470427	Approved	Completed	ModernaTX, Inc.	2
mRNA-1345	Stabilized prefusion F glycoprotein of RSV	RSV-associated lower respiratory tract disease in adults ≥60 years old	SM102, cholesterol, DSPC, DMG-PEG 2000	Intramuscular injection	50 μg	NCT07117487	Approved	Completed	ModernaTX, Inc.	3
SYS6006	Prefusion stabilized full-length spike protein	COVID-19	Ionizable lipid, DSPC, cholesterol, etc.	Intramuscular injection	20 μg	ChiCTR2200066941	Approved	Completed	CSPC pharmaceutical group limited	4
RQ3033	Full-length spike protein of omicron XBB.1.5 variant	COVID-19	Ionizable lipid, DSPC, cholesterol, DMG-PEG 2000	Intramuscular injection	Undisclosed	ChiCTR2300077397	Approved	Completed	Walvax Biotechnology, Fudan University, Shanghai RNACure Biopharma	–
mRNA-1647	CMV pentamer complex and glycoprotein B protein	Cytomegalovirus infection	SM102, cholesterol, DSPC, DMG-PEG 2000 = 50:38.5:10:1.5	Intramuscular injection	100 μg	NCT05085366	III	Active, not recruiting	ModernaTX, Inc.	5
mRNA-1010	Membrane-bound hemagglutinin (HA) surface glycoproteins of four influenza strains	Seasonal influenza	Undisclosed	Intramuscular injection	50 μg	NCT06602024	III	Completed	ModernaTX, Inc.	6,7
mRNA-1440 (VAL-506440)	HA sequence of H10N8	Influenza A	Undisclosed	Undisclosed	Undisclosed	NCT03076385	I	Completed	ModernaTX, Inc.	–
DCVC H1 HA mRNA vaccine	Full length HA of influenza A/California/07/2009 (H1N1)	Influenza	Ionizable lipid, DSPC, cholesterol, and PEG-lipid	Intramuscular injection	10, 25, and 50 μg	NCT05945485	I	Active, not recruiting	NIAID	–
H1ssF-3928	Undisclosed	Influenza	ALC307 (ionizable lipid), DSPC, cholesterol, and ALC0159	Intramuscular injection	10, 25, and 50 μg	NCT05755620	I	Active, not recruiting	NIAID	–
mRNA-1083	Antigens from SARS-CoV-2 and seasonal influenza strains	Influenza and COVID-19	Undisclosed	Intramuscular injection	40 μg	NCT06097273	III	Completed	ModernaTX, Inc.	8
JCXH-108	Prefusion F protein of RSV	RSV	Undisclosed	Intramuscular injection	Undisclosed	NCT06564194	I	Active, not recruiting	Immorna Biotherapeutics, Inc.	–
SYS6016	Prefusion F protein of RSV	RSV	Undisclosed	Undisclosed	Undisclosed	ChiCTR2400091478	I	Not yet recruiting	CSPC pharmaceutical group limited	–
STR-V003	Prefusion F protein of RSV	RSV	Undisclosed	Intramuscular injection	Undisclosed	NCT06344975	I/II	Not yet recruiting	Starna therapeutics	9
mRNA-1189	EBV envelope glycoproteins	Epstein-Barr virus (EBV)	Undisclosed	Intramuscular injection	Undisclosed	NCT05164094	I/II	Active, not recruiting	ModernaTX, Inc.	–
mRNA-1195	Undisclosed	EBV	Undisclosed	Intramuscular injection	Undisclosed	NCT05831111	I	Active, not recruiting	ModernaTX, Inc.	–
mRNA-1644	eOD-GT8 60mer	Human Immunodeficiency virus (HIV)	Undisclosed	Intramuscular injection	100 μg	NCT05001373	I	Active, not recruiting	International AIDS vaccine Initiative	–
mRNA-1644v2-core	Core-g28v2 60mer	HIV	Undisclosed	Intramuscular injection	100 μg	NCT05001373	I	Active, not recruiting	International AIDS vaccine Initiative	–
mRNA-1325	Premembrane and envelope E structural proteins from a Micronesia 2007 ZIKV isolate	Zika virus (ZIKV)	Undisclosed	Intramuscular injection	10, 25, and 100 μg	NCT03014089	I	Completed	ModernaTX, Inc.	10

(*continued on next page*)

Table 1 (*continued*)

Product Name	Antigen/protein	Disease	LNP composition	Administration route	Dose	Trial Number	Phase	Status	Sponsor	Ref.
mRNA-1893	Premembrane and envelope E structural proteins from the RIO-U1 ZIKV isolate	ZIKV	Undisclosed	Intramuscular injection	10, 30, 100, and 250 μg	NCT04917861	II	Completed	ModernaTX, Inc.	11
IN001	Undisclosed	Herpes zoster	Undisclosed	Intramuscular injection	Undisclosed	NCT06375512	I	Active, not recruiting	Shenzhen Shenxin Biotechnology co., Ltd.	–
BNT164a1 and BNT164b1	Undisclosed	Tuberculosis	Undisclosed	Intramuscular injection	Undisclosed	NCT05537038	I	Active, not recruiting	BioNTech SE	–
BNT165b1	Part of the plasmodium falciparum circumsporozoite protein	Malaria	Undisclosed	Intramuscular injection	3, 10, and 30 μg	NCT05581641	I	Completed	BioNTech SE	–
mRNA-1944	Chikungunya virus-specific monoclonal neutralizing antibody	Chikungunya virus	Undisclosed	Intravenous injection	0.1, 0.3, and 0.6 mg/kg	NCT03829384	I	Completed	ModernaTX, Inc.	–
Cancer										
mRNA-4157 (V940)	Up to 34 personalized neo-antigens derived from the patient's tumor mutational signature	V940 plus pembrolizumab: Melanoma, non-small cell lung cancer, Renal cell carcinoma, Bladder cancer V940 plus bacillus calmette-guerin: bladder cancer	Undisclosed	Intramuscular injection	1 mg every 3 weeks for up to 9 doses	NCT05933577 (III, active, not recruiting) NCT06623422 (III, recruiting) NCT06307431 (II, active, not recruiting) NCT06305767 (I/II, recruiting) NCT06833073 (II, recruiting)			Merck sharp & Dohme LLC	12
BNT113	Human Papillomavirus (HPV) 16 E6 and E7 oncoproteins	HPV16 positive head and neck squamous cell carcinoma that expresses PD-L1	Undisclosed	Intravenous injection	Undisclosed	NCT04534205	II/III	Recruiting	BioNTech SE	13
RG002	Undisclosed	HPV 16 or 18 associated cervical intraepithelial neoplasia grade 2 or 3	Undisclosed	Intramuscular injection	25, 75, and 150 μg	NCT06273553	I/II	Not yet recruiting	RinuaGene Biotechnology co., Ltd.	–
ARC01	HPV-16 E6/E7 antigens	HPV16-positive advanced unresectable or recurrent/metastatic solid tumors	Undisclosed	Intravenous administration	Undisclosed	ChiCTR2400092093	I	Recruiting	GrandPharma (China) co., Ltd.	–
ABO2011	Human interleukin-12	Advanced solid tumors	Undisclosed	Intratumoral injection	Undisclosed	NCT06088004	I/II	Recruiting	Suzhou Abogen Biosciences co., Ltd.	14
JCXH-211	Human interleukin-12	Malignant solid tumors	XH-07, cholesterol, DSPC, DMG-PEG 2000 = 40:48:10:2	Intratumoral injection	Undisclosed	NCT06781125	I	Not yet recruiting	Immorna Biotherapeutics, Inc.	15
STX-001	Human interleukin-12	Advanced solid tumors	Undisclosed	Intratumoral injection	Undisclosed	NCT06249048	I/II	Recruiting	Strand therapeutics Inc.	–
EVM16	Patient-specific tumor neoantigens	Solid tumors	Undisclosed	Undisclosed	Undisclosed	NCT06541639	I	Recruiting	Everest Medicines	–
InnoPCV	Individualized neo-antigen	Advanced solid tumors	Undisclosed	Intramuscular injection	0.06−1 mg, every 3 weeks	NCT06497010	Early phase I	Recruiting	Innovac therapeutics	–
Other disease										
ARCT-032	Cystic fibrosis transmembrane conductance regulator	Cystic fibrosis	Lunar® platform	Inhaled	Undisclosed	NCT06747858	II	Recruiting	Arcturus therapeutics, Inc.	16
MRT5005	Cystic fibrosis transmembrane conductance regulator	Cystic fibrosis	Undisclosed	Nebulization	8, 12, 16, 20, and 24 mg	NCT03375047	I/II	Unknown	Translate Bio, Inc.	17
ARCT-810	Ornithine transcarbamylase	Ornithine transcarbamylase deficiency	Undisclosed	Intravenous injection	Undisclosed	NCT06488313	II	Recruiting	Arcturus therapeutics, Inc.	–

YOLT-201	Undisclosed	Transthyretin amyloidosis cardiomyopathy	Undisclosed	Intravenous injection	Undisclosed	NCT06082050	Early phase I	Recruiting	Yoltech therapeutics	–
mRNA-3705	Methylmalonyl-CoA mutase	Methylmalonic acidemia	SM-86, DSPC, cholesterol, OL-56 (PEG-lipid)	Intravenous injection	0.1 mg/kg every 3 weeks; 0.2, 0.4 and 0.6 mg/kg every 2 weeks	NCT04899310	I/II	Recruiting	ModernaTX, Inc.	18,19
mRNA-3927	Propionyl-coenzyme A carboxylase α and β subunit	Propionic acidemia	SM-86, DSPC, cholesterol, OL-56 (PEG-lipid)	Intravenous injection	0.3 mg/kg every 3 weeks; 0.3, 0.45, 0.6 and 0.9 mg/kg every 2 weeks	NCT04159103	I/II	Recruiting	ModernaTX, Inc.	20,21
ABO2203	CD19/CD3 T cell engager	Refractory autoimmune diseases	Undisclosed	Subcutaneous injection	Undisclosed	NCT06747156	Early phase I	Recruiting	Suzhou Abogen Biosciences co., Ltd.	–
SYS6020	Chimeric antigen receptor (CAR) targeting B-cell maturation antigen	Refractory active systemic lupus erythematosus	Undisclosed	Intravenous infusion	Undisclosed	NCT06694298	I	Not yet recruiting	CSPC pharmaceutical group Ltd.	–
		Myasthenia gravis		Undisclosed	$2 \cdot 10^6$–$5.4 \cdot 10^7$ CAR + T cells per kg	NCT06688435	I	Recruiting		
		Multiple myeloma		Intravenous infusion	Undisclosed	NCT06359509	Early phase I	Not yet recruiting		

film hydration and ethanol injection are the primary traditional bulk production methods for LNP[39]. However, these methods generally fail to properly control the self-assembly process of nanoparticles, leading to unstable quality and significant batch-to-batch variation. Microfluidic mixing, currently the predominant method for mRNA-LNP preparation, ensures superior reproducibility and robust process control[40,41]. Advanced microfluidic systems such as staggered herringbone micromixers, bifurcating mixers, baffle mixers, and T-junction mixers[42-44] have well-documented applications and optimization strategies[44-47].

While microfluidic platforms have significantly advanced LNP development, these systems are typically chip-based with relatively low throughput. To overcome this limitation, studies have employed parallelized microfluidics to scale up production[44,48]. However, careful consideration should be given to solvent compatibility of the devices (especially with organic reagents) and potential clogging or fouling issues[44]. Confined impinging jet reactors represent another method for preparing mRNA-LNPs, enabling efficient and rapid mixing of mRNA and lipid components through impinging jets. They offer higher throughput, making them suitable for large-scale production[49].

Post-encapsulation is another preparation technique under development[50]. Tanaka et al.[51] prepared empty LNP separately and then completed the preparation of mRNA-LNPs by mixing mRNA with these LNPs under optimized pH conditions. Furthermore, the strategy is particularly suitable for small-scale mRNA-LNPs preparation, offering a practical method for rapidly screening multiple mRNAs or LNPs[52]. SMART (Sprayed Multi Absorbed-droplet Reposing Technology) platform, integrated with multi-channel guided internal-control printheads, constitutes an innovative fabrication technique that is expected to enable precise control over LNP size[53].

Inhalable formulations, including liquids and powders, are commonly used for mucosal administration. Powder formulations exhibit greater stability compared to liquid formulations. Sarode et al.[54] presented the preparation of mRNA-LNP powder formulations by spray drying. This process requires the addition of excipients and involves heating for drying. To avoid the impact of heat during preparation on mRNA functionality, another study developed a novel spray freeze-drying technique with adding a pH modifier. The resulting mRNA-LNPs maintained their functionality following 62 days of storage, which is conducive to promoting their widespread application[55].

3. Biodistribution of mRNA-LNPs

The biodistribution of mRNA-LNPs can be differentially influenced by multiple factors, including LNP compositions, particle size, surface characteristics (*e.g.*, surface charge and chemical modifications), dose, and administration routes, which collectively affect their efficacy and safety profiles. Although isotopic and fluorescent labeling techniques are widely used to track mRNA-LNP biodistribution, the dynamic interplay between nanoparticle disassembly and tissue-specific accumulation remains incompletely characterized, leaving critical knowledge gaps in our understanding of this field.

From an analytical perspective, ideally, each LNP component requires individual testing. Only by integrating tissue and cellular co-localization data for every component can one truly determine whether a specific component can act as a representative surrogate for the entire LNP. However, most studies focus solely on a single

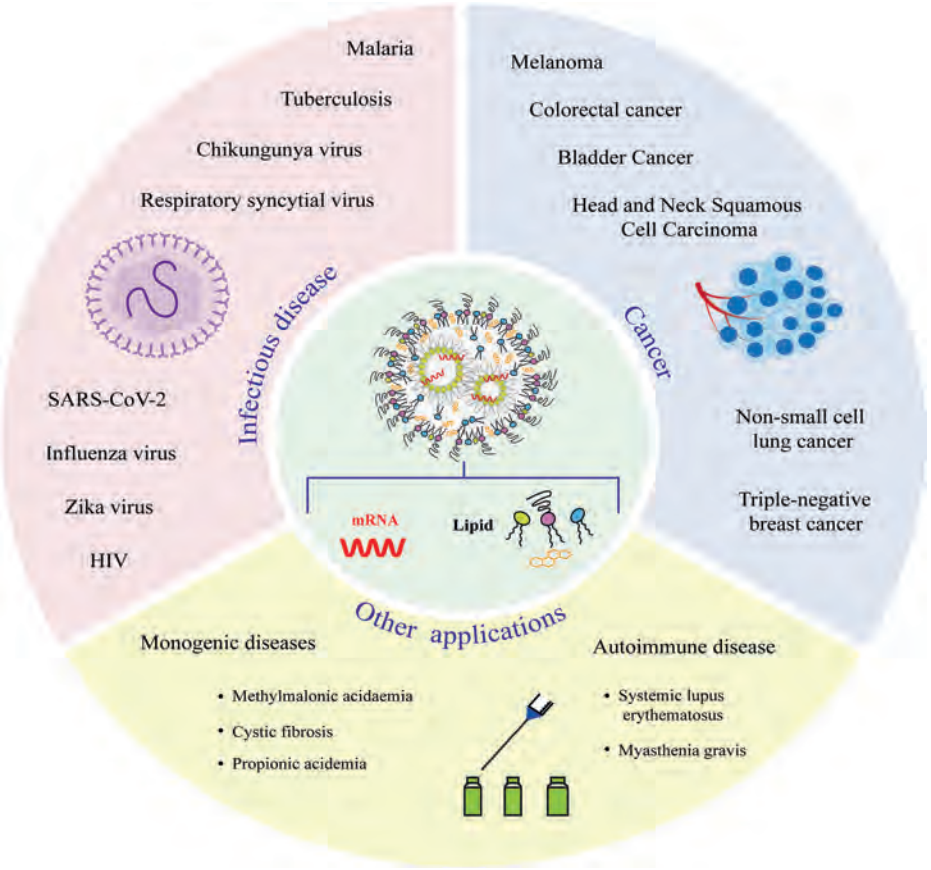

Figure 1 Representative mRNA-LNP-based biologics and their relevant indications.

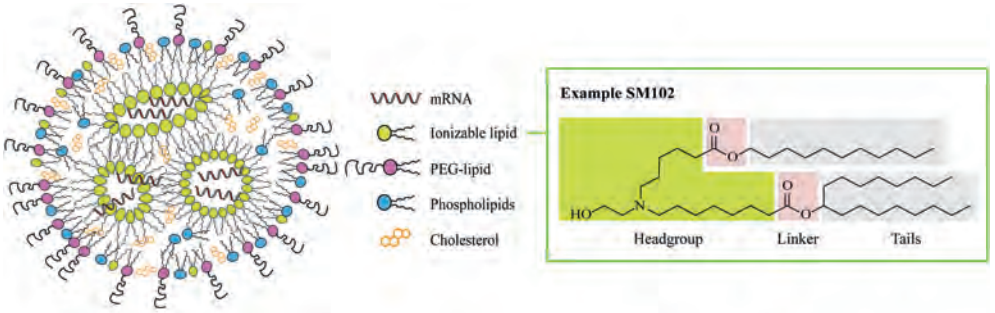

Key lipids	Key element	Regulated LNP properties	Effects on the *in vivo* fate
Ionizable lipid	Headgroup	Formulation stability, internal structure	Biodistribution, interacting with the membrane, endosomal escape
	Linker	Formulation stability, biodegradability, cytotoxicity	The clearance and transfection efficiency
	Tails	Fluidity, fusogenicity, formulation stability	Biodistribution, endosomal escape and transfection efficiency
PEG-lipid	PEG chain	Surface properties	The interaction with protein, cellular uptake
	Lipid anchors	Formulation stability	The desorption rate of PEG-lipid, cellular uptake, biodistribution
	Amount	Formulation stability	Translation efficiency, circulation time
Phospholipids	Tails	Formulation stability	Endosomal escape, transfection efficiency, biodistribution
	Headgroup	Formulation stability	
Cholesterol	Derivatives	Formulation stability, internal structure	Endosomal escape

Figure 2 Chemical structure of mRNA-LNPs (nanostructured core−shell architecture) and the impact of components on LNP properties and *in vivo* fate.

component within LNPs or the target protein encoded by the loaded mRNA. Therefore, the following discussion will address evidence-supported distributions of LNP components, rather than presuming to describe the entire mRNA-LNP biodistribution as frequently claimed in many studies.

3.1. Biodistribution of lipids

Comparative studies reveal tissue-specific distribution patterns. An early head-to-head analysis of mRNA-LNPs containing different ionizable lipids (MC3 and novel lipids) in CD-1 mice showed that intramuscularly administered ionizable lipids were mainly localized at the injection site, with secondary accumulation in the liver and spleen[56]. Exogenous-lipid biodistribution data highlight elimination differences. Following intravenous (IV) administration of mRNA-LNP (1 mg/kg) in Wistar Han rats, ionizable lipid ALC0315 exhibited approximately 60% hepatic distribution of the administered dose, with peak concentrations reaching 294 μg/g liver tissue at 3 h. ALC0315 exhibited slow hepatic elimination, retaining ∼25% of its peak concentration at 2 weeks, indicating complete clearance from rat liver requires ∼6 weeks. Conversely, PEG-lipid ALC0159 showed ∼20% hepatic distribution, peaking earlier at 15.2 μg/g liver tissue within 30 min and declining rapidly to ∼0.04% residual levels after 2 weeks[57]. Compared to ALC0315, ALC0159 exhibits reduced hepatic accumulation and accelerated elimination kinetics. This divergence may stem primarily from its lower molar ratio compared to ionizable lipids in the LNP formulation, coupled with rapid dissociation of PEG-lipids. Crucially, the biodistribution of ionizable lipids may more closely approximate that of LNPs, as ionizable lipids predominantly localize within the LNP core. However, extrapolating the distribution of lipid components to represent LNP biodistribution requires cautious interpretation, as the detected signals may not reflect intact lipids/LNPs due to metabolic elimination, structural disassembly, or exocytosis post-uptake.

Deuterated cholesterol is known for its safety, high sensitivity, and strong specificity. Using liquid chromatography-tandem mass spectrometry (LC−MS/MS) technology, its concentration changes in various tissues can be accurately quantified. However, the application of deuterated cholesterol as an LNP marker depends on the critical assumption that LNP remains structurally intact without undergoing disassembly or cholesterol lipid exchange *in vivo*. This assumption can be validated by simultaneously labeling other LNP components (*e.g.*, ionizable lipids or PEG-lipids) and analyzing the discrepancies in their distribution patterns. Due to insufficient evidence, this review centers exclusively on the *in vivo* distribution of deuterated cholesterol after mRNA-LNP administration.

Di et al.[58] documented that following intramuscular (IM) injection of mRNA-LNP, deuterated cholesterol signals were detectable in the mouse blood within 30 min, peaking at 2 h and gradually declining thereafter, yet persisting at detectable levels even 24 h post-injection. The deuterated cholesterol detected in the blood accounted for approximately 15% of the total injected dose. This distribution pattern could suggest either rapid entry of intact mRNA-LNP into systemic circulation or release of deuterated cholesterol caused by LNP disassembly before entering the bloodstream. In addition, the tissue with the highest content of deuterated cholesterol was the muscle at the injection site, accounting for approximately 60%−80% of the administered dose, followed by the liver (10%−20%) and spleen (about 1%−2%). These findings are broadly consistent with the *in vivo* distribution characteristics of the LNP-encapsulated fluorescent dye DiR. The observed similarity could result from their shared characteristic of strong hydrophobicity and/or the co-encapsulation of these compounds within LNPs.

3.2. Biodistribution of mRNA

The distribution of mRNA can be qualitatively observed *via* RNA probe *in situ* hybridization (ISH)[58]. Di et al.[58] detected mRNA in local injection-site muscle, liver, and draining lymph node tissues by employing Cy5-labeled probes targeting mRNA sequences. Additionally, fluorophore-labeled mRNA, synthesized *via in vitro* transcription from nucleotide components, enables direct application in *in vivo* distribution studies. Chen et al.[59] used Cy5-labelled mRNA to investigate the tissue distribution of SM102-based mRNA-LNP administered *via* IM. Interestingly, fluorescent signals were found to disseminate mainly to the liver rather than the muscle (6 h after administration), indicating that mRNA-LNP can distribute from the local injection site to systemic circulation and therefore distal organs in a short period of time upon IM administration. However, it remains unclear whether the particles migrate directly from the injection site to systemic circulation, or first to lymphatic tissue before entering systemic circulation. Other distal tissues, such as the spleen, showed mRNA-LNP distribution, which had a similar distribution level as muscle. Given that SM102-based LNP has been successfully utilized in COVID-19 vaccines administered intramuscularly, its concentrated distribution at the injection site might not be critical for triggering an immune response. Understanding the distribution at the cellular level, particularly within immune cells, is essential to decipher how mRNA distribution contributes to vaccine efficacy.

mRNA can be quantified to study its distribution when being delivered by LNP[60-62]. Bahl et al.[63] applied branched DNA (bDNA) to study mRNA distribution delivered in LNP following IM administration in mice. They found that mRNA was most abundant in muscle tissue, followed by proximal lymph nodes. Additionally, distal lymph nodes, the liver, and spleen also showed significant distribution. This is an important finding as it reveals the *in vivo* process of mRNA-LNP transferring from the injection site to systemic circulation *via* the lymphatic system. While the biodistribution of mRNA is more meaningful for immunization or therapy than that of the lipid, it is noteworthy that mRNA distribution within specific tissues or cells does not guarantee functional protein translation. Indeed, it has been observed that mRNA can be internalized by certain cell types without subsequent protein expression[60].

4. Key factors influencing the distribution of expressed protein

The abundance of mRNA-encoded proteins can be quantified *via* ELISA, while their spatial distribution can be mapped directly by luciferase-based bioluminescence imaging. Notably, protein expression patterns do not mirror mRNA-LNP biodistribution due to dynamic processes like LNP disassembly, cellular uptake, intracellular degradation, exocytosis, and tissue-specific translational efficiency.

For IV delivery, MC3-based mRNA-LNP exhibited higher protein (EGFP) expression in the liver than the spleen in mice[61].

Li et al.[64] demonstrated higher luciferase expression in the liver than the spleen following IV delivery of luciferase mRNA *via* MC3-based mRNA-LNP. The distribution ratio of liver/spleen was about 5−20, depending on the nitrogen-to-phosphate ratio[64]. It is worth noting that the liver/spleen ratio of distribution (evaluated by translated protein) *via* IV injection is much higher than the ratio (about 1, quantified by lipid amount) *via* IM injection[56]. The difference arises from the combined effect of administration route, dose injected or disseminated into circulation, and quantification methodology.

Intramuscular injection of MC3-based mRNA-LNP revealed distinct biodistribution patterns, as assessed by luciferase expression. At the 4.5-h time point, muscle was identified as the primary site of distribution, with expression levels higher than those observed in the liver[65]. This distribution pattern in tissues is consistent with that evaluated in lipid amount by mass spectrometry (from 1 to 24 h)[56]. Notably, significant accumulation was also observed in the liver, which aligns with the well-established hepatic tropism of MC3-based LNPs following IV infusion. Understanding the tissue distribution profile—across muscle, liver, and spleen—is crucial for guiding the rational design of novel lipids for diverse clinical applications. To expand mRNA-LNP therapeutics beyond infectious diseases, developing formulations that enhance extrahepatic delivery remains paramount.

Furthermore, Bahl et al.[63] found that the distribution of bioluminescence from mRNA-expressed protein followed the order of muscle, liver, spleen at various doses (2, 0.4, and 0.08 μg) when imaged at 6 h post IM administration. With a closer examination, the skin and lymph node were rich in bioluminescence, which might be associated with adjacent location to the injection site of muscle. It is worth noting that the above spread, as seen from the mRNA-expressed protein, differed from that as quantified from mRNA itself, which followed the order of muscle, proximal lymph node, spleen, and liver[63]. The difference could come from various factors such as the size of tissues, different biological processes, variety of cells, translational capabilities of cells, various determination methodologies, resolution of methods, etc. Notably, Carrasco et al.[66] reported liver-dominant protein expression (*vs.* muscle) for IM-injected *Fluc*-mRNA MC3-LNP at 4- and 24-h time points. This discrepancy may stem from LNP composition, physicochemical properties, injection parameters (volume/depth), or distribution kinetics.

These findings highlight the complex *in vivo* fate of mRNA-LNPs, encompassing lymphatic transport, systemic circulation, and extensive tissue distribution. Moreover, they emphasize multifactorial influences on protein distribution patterns, including administration routes, LNP formulation, tissue tropism, and methodological discrepancies (Fig. 3). The key contributing factors are discussed below.

4.1. Impact of LNP composition on the distribution of expressed proteins

4.1.1. Cholesterol and phospholipids

Cholesterol content in mRNA-LNP critically modulates protein expression. For example, under conditions where the molar percentages of PEG-lipid and ionizable lipid remain constant, increasing the cholesterol molar percentage from 10% to 40% while reducing the proportion of helper lipid DOPC resulted in significantly elevated luciferase expression levels in the mouse liver following IM injection of SS-OP or MC3-based mRNA-LNP[65]. Notably, this formulation adjustment did not substantially alter luciferase expression in muscle at the local injection site. Intriguingly, when administered subcutaneously, a cholesterol molar percentage-dependent enhancement of protein expression was also observed in the local tissue at the injection site[65]. Similar phenomena were also observed in *in vitro* HepG2 cells. Although researchers ruled out the effects of particle size and zeta potential

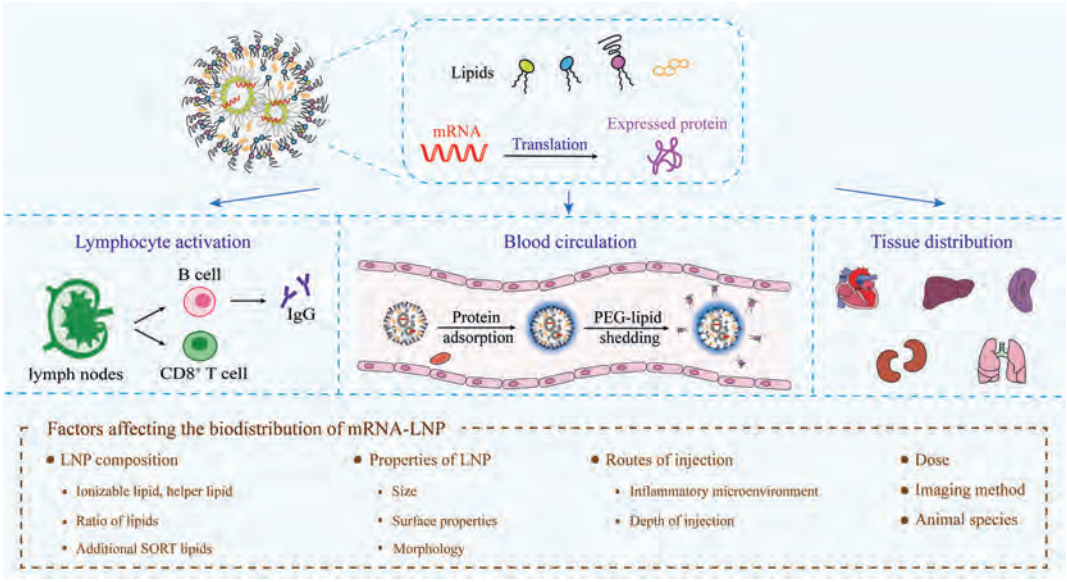

Figure 3 The processes of mRNA-LNP *in vivo* and factors influencing their biodistribution. After administration, mRNA-LNP can be transported to lymph nodes, activating immune cells; it can also enter the blood circulation, generating a biomolecular corona on its surface, while PEG-lipids could be shed, thus leading to morphological changes. mRNA-LNP in circulation will be widely distributed in various tissues and organs. There are many factors affecting the mentioned processes (especially biodistribution), mainly including: LNP composition (ionizable lipids, helper lipids, component ratio, additional selective organ targeting (SORT) lipids, etc.), LNP properties (size, surface properties, morphology, etc.) administration routes (inflammatory microenvironment, injection depth), dose, and imaging methods, and animal species etc.

of mRNA-LNP, the observed phenomena are likely attributable to alterations in surface lipid distribution characteristics and internal structural reorganization of LNP induced by modified cholesterol/DOPC molar ratios. Critically, surface lipid redistribution may alter the protein corona composition, consequently affecting circulation stability, tissue/cellular tropism, and their interactions.

4.1.2. Ionizable lipids

Ionizable lipids dictate tissue tropism. Long et al.[67] discovered that following IM injection, the bioluminescent signals mediated by MC3-based LNPs were primarily localized in the liver; whereas YK009-based LNPs showed predominant distribution at the injection site and in the spleen. It is reported that SM102-based LNP shows broad tissue dissemination (muscle > liver > spleen, evaluated as Fluc-mRNA expression at 6 h post-IM[59]. Given the wide distribution in various tissues, which causes side effects in off-target tissues, a novel ionizable lipid iso-A11B5C1 was designed to dissipate mainly in the injection site. Truly, the majority of Fluc-mRNA expression was detected in the muscle with little expression in liver, spleen, lymph node, antigen presenting cells post IM administration in mice[59]. In view of this interesting muscle tropism, immune elicitation was further studied. Interestingly, although limited mRNA expression in lymph node and immune cells, iso-A11B5C1-based mRNA-LNP elicited a potent cellular response and prominent therapeutic efficacy as a cancer vaccine in a melanoma model[59]. This study reveals that a specific distribution in muscle could be sufficient to elicit an immune response, which provides insight into designing effective vaccines with minimal off-target and side effects.

Lam et al.[61] investigated the distribution of mRNA-expressed protein delivered by various ionizable lipid-based LNPs that are used in clinical trials or have been marketed, such as MC3, Lipid 10, SM102, and ALC0315 (Fig. 4). At 6 h post-IM injection, luciferase protein expression was detected at the injection site. The total bioluminescent signal in the muscle was comparable among Lipid 10-, SM102-, and ALC0315-based LNPs but approximately two-fold higher than that of MC3-based LNPs. Furthermore, the study found that after IV injection, SM102-based LNPs loaded with EGFP mRNA showed no significant hepatic expression, whereas ALC0315-based LNPs exhibited significantly higher expression in the spleen compared to SM102-based LNPs.

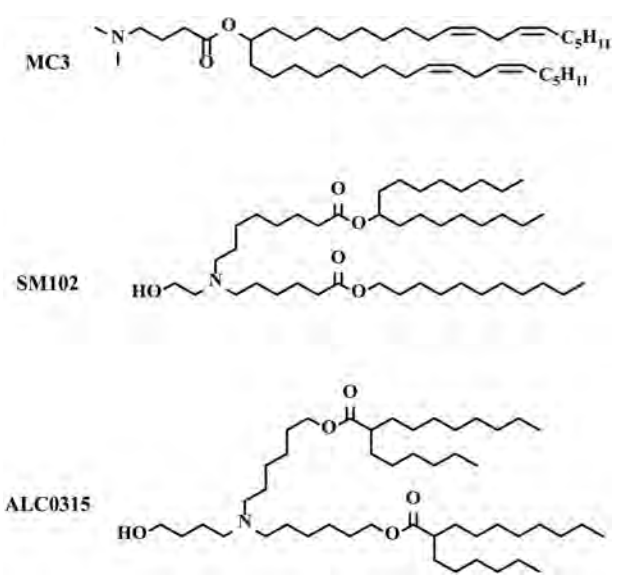

Figure 4 The ionizable lipids are employed in Comirnaty® (ALC0315) and Spikevax® (SM102), as well as in Onpattro (MC3).

Given the critical role of ionizable lipids in mRNA-LNP delivery, numerous studies have synthesized a range of ionizable lipids with varying lengths, headgroups numbers, and tail chains numbers to investigate their effects on tissue distribution. For example, Hashiba et al.[68] examined how the branched chain length of ionizable lipids influences the biodistribution of expressed protein after IV injection in mice. Results demonstrated that as the lipid tail length shortened, the luciferase expression pattern gradually transitioned from the liver to the spleen.

4.1.3. Ratios of lipids

The molar ratios of individual lipids represent a decisive parameter in LNP formulations, directly influencing nucleic acid delivery efficiency, biodistribution and protein expression patterns. One study demonstrated that whether administered *via* intramuscular or subcutaneous injection, luciferase expression levels in the liver decreased in conjunction with reduced cholesterol levels[65]. Another study investigated the biodistribution profiles of expressed protein with increased DSPC molar percentages. The results demonstrated that after IV administration, compared to the reference formulation (10% DSPC), luciferase expressed by LNPs with elevated DSPC levels (30%) exhibited a pronounced biodistribution preference in the inflamed colon, concurrently with diminished accumulation in the liver and spleen[69]. Furthermore, the optimal lipid ratios of LNPs vary across different administration routes. Reducing the molar concentration of DMG-PEG from 1.5% to 0.5% markedly enhances luciferase protein expression in the lungs at 6 h post intratracheal administration in mice[70].

4.2. Impact of LNP properties on the distribution of expressed protein

4.2.1. Size

Particle size is a critical parameter influencing mRNA delivery efficiency and biodistribution. Cui et al.[71] compared MC3-based LNP with identical composition but differing hydrodynamic diameters achieved through process parameter adjustments. Larger LNPs exhibited stronger hepatic mRNA expression (bioluminescence, 24 h post-IV) and broader white adipose tissue distribution compared to smaller counterparts. Mechanistic studies established that larger lipid nanoparticles enhance mRNA delivery by accommodating greater payload capacities.

4.2.2. Surface charge

Traditional mRNA-LNPs are engineered to be electrically neutral at physiological pH, a key design feature that enhances their systemic stability and safety profile. However, their surface charge can be modulated by introducing a fifth charged lipid. The modified surface charge can substantially modulate the biodistribution of expressed protein. Cheng et al.[72] incorporated a fifth lipid, either 1,2-dioleoyl-3-trimethylammonium-propane DOTAP (positive) or 1,2-dioleoyl-*sn*-glycero-3-phosphate (18 PA) (negative), to LNP formulations to manipulate the overall charge property of LNPs. By supplement DOTAP in MC3 standard formulations, the expression of payload luciferase mRNA declined in the liver but increased in the lung (for IV). Notably, positively charged lipids demand cautious application to mitigate potential adverse effects associated with overuse. Similarly, when negatively charged 18 PA is incorporated into the LNP formulation, it enables the luminescence

signal to be primarily distributed in the spleen. In another study, the inclusion of the cationic lipid IM21.7c into a DODMA-based LNP formulation resulted in nanoparticles that, upon intravenous administration, exhibited preferential distribution to the lungs, as assessed by luciferase expression[73].

4.2.3. Morphology and internal microstructure of mRNA-LNP

The morphology and internal microstructure of LNPs, a key determinant of encapsulated mRNA integrity and delivery efficiency, can be characterized by cryogenic transmission electron microscopy, scattering techniques, or fluorescence microscopy[74-77]. The variations in lipid composition—particularly in the content and molecular structure of cholesterol—significantly influence LNP structure. Eygeris et al.[37] determined the pivotal role of cholesterol derivative variants in regulating LNP architecture. LNPs composed of conventional cholesterol primarily form unilamellar structures, while β-sitosterol induces polymorphic shape and increases the proportion of multilamellar membranes. Notably, β-sitosterol-based LNPs exhibit higher transfection efficiency in HeLa cells than cholesterol-based LNPs.

The ratio of bilayer-forming lipids within LNPs directly impacts internal structure and biodistribution. Cullis and colleagues investigated the properties of mRNA-LNP systems with high proportions of bilayer lipids (egg sphingomyelin and cholesterol). As the molar ratio of bilayer lipids to ionizable lipids reached 4, the system displayed a liposomal morphology, characterized by a solid core suspended inside an aqueous interior enclosed by a lipid bilayer. Upon intravenous injection, these liposomal LNPs (^{111}In-labelled) showed a prolonged circulatory half-life[78]. *In vivo* Imaging System (IVIS) revealed the preferential distribution of the formulation to lymph nodes and pancreas, as indicated by the nanoLuc luminescence signal, demonstrating enhanced extrahepatic transfection potency. Further studies with increased sample sizes or alternative animal models are necessary to confirm these findings.

LNPs are typically characterized by surface properties such as average particle size, polydispersity index, and surface zeta potential. In contrast, few studies systematically investigate the relationship between internal structure and protein expression/biodistribution—partially due to the challenges in interpreting spectroscopic results. Wu et al.[79] prepared three types of LNPs with distinct internal structures: emulsion-like LNPs, membrane-rich LNPs, and classic "bleb" structure LNPs, and compared their biodistribution and immune effects. Results showed that compared with other LNPs, the encoded luciferase signal of emulsion-like LNPs primarily remained at the injection site post IM injection, provoking faster onset and longer-lasting immune responses. Notably, these three LNP structures were obtained by adjusting lipid ratios, and they also exhibited differences in particle size and zeta potential. Therefore, further exploration is needed to establish a direct correlation between LNP internal structure and biodistribution/functional effects.

4.3. Administration routes

Vaccination against infectious diseases is generally administered locally. Among the widely applied routes of administration, IM and subcutaneous (SC) injections are valued for their convenience, while intradermal (ID) injection has dose-sparing potential. The microenvironment of different injection sites, such as the spatial size, the types and abundance of resident cells, and the local protein expression capacity, affects protein expression and immune potency.

The injection site of ID is in the dermis of skin, where many antigen-presenting cells (APCs) are present to internalize and process mRNA and mRNA-encoded antigens. APCs in the dermis, such as Langerhans cells (LC), can take up and present antigens followed by migrating to draining lymph nodes and activating lymphatic T cells. In these processes, mRNA-LNPs and mRNA-encoded antigens can be transported by LC to the draining lymph nodes. Besides, it is conceivable that mRNA-LNP and mRNA-encoded antigen are passively carried to lymph nodes through blood vessels or lymphatic vessels, where they could facilitate their exposure to immune cells, ultimately resulting in the activation of T and B cells[80]. Compared to dermis, subcutaneous tissue contains fewer immune cells and more adipose tissue, which leads to less pain during administration, but a generally compromised immune response activation. Muscle is a tissue below the subcutaneous layer and contains a relatively large vascular network capable of rapidly recruiting APCs to injection sites. It is found that mRNA and mRNA-translated protein were present in the infiltrating immune cells at the intramuscular injection site[60]. Besides, APCs and mRNA-LNPs migrated to the draining lymph nodes to activate an immune response, with macrophages showing high protein expression[60].

Following IM, SC, and ID administrations, the expressed proteins are primarily distributed in local injection sites[63,65,81]. Qiu et al.[82] applied bioluminescence imaging (BLI) to assess the impact of delivery routes on the distribution of expressed protein in mice. Results showed that IV led to broad distribution in organs including the liver, spleen, lung, and lymph nodes; in contrast, SC resulted in luciferase expression restricted to lymph nodes. Besides, the depth of injection impacts expressed protein distribution. Superficial IM injection mainly leads to muscle expression, whereas deep IM injection produces most protein in the liver[81].

4.4. Dose

Dose affects local or distal distribution. Bahl et al.[63] utilized BLI to investigate the dose-dependent biodistribution of luciferase-mRNA-LNPs. Findings demonstrated that low doses of mRNA-LNPs exhibited distribution in local tissues such as muscle and skin when administered *via* IM and ID routes. In contrast, high doses of mRNA-LNPs lead to distal distribution in spleen and liver, etc. This interesting dissemination is most likely related to the limited capacity at the injection site and a high diffusion rate of mRNA-LNPs to the surrounding tissues and distal tissues at high concentration. Meanwhile, cellular uptake at the injection site can be saturated at high particle concentration, facilitating distal spreading.

5. Cellular uptake, endosomal escape, and distribution of mRNA-LNPs

Although mRNA-LNPs administered *via* various routes distribute systemically to various tissues, the specific cell types that take up these particles—a key factor that dictates both protein expression and therapeutic efficacy (*e.g.*, immune activation)—remain unidentified to date. Hassett et al.[60] investigated the distribution of mRNA from SM102-based mRNA-LNPs and the protein it expresses, within muscle and lymph nodes at both tissue and cellular levels. At the intramuscular injection site in non-human primates (NHPs), analysis revealed that the mRNA and its encoded EGFP protein were distributed in macrophages, fibroblasts, and

intermuscular adipocytes. Interestingly, neither mRNA nor protein expression was found in muscle fibers. In lymph nodes of mice, most mRNA was eliminated from the lymph nodes, with residual mRNA localized in B cell follicles and interfollicular regions[60]. However, the encoded EGFP protein was primarily localized in macrophages residing in subcapsular and medullary sinuses. Besides, EGFP expression was minimal in the left popliteal lymph node (5%), with negligible levels in the contralateral popliteal and bilateral inguinal nodes; this variability may be related to the inconsistent tissue collection and the distance from the injection site[60]. Notably, protein expression varied throughout the tissue, even within the iliac lymph nodes. The above results suggest that the inhomogeneous distribution of LNP within target tissue may cause uneven cellular uptake. This, in turn, results in inconsistent protein translation, which can cause variable biological effects. Therefore, studying the cellular distribution and intracellular fate of mRNA-LNPs is essential.

5.1. *Cellular uptake mechanisms*

After intracellular delivery, mRNA ends up in the cytoplasm, where it is translated into the target protein. Clathrin-mediated endocytosis (CME) is reported to be the primary pathway mediating the entry of LNPs into cells. Clathrin forms a triskelion scaffold *via* three heavy and three light chains[83,84]. Gilleron et al.[27] discovered that heavy chain downregulation reduces LNP uptake by ∼50%, confirming CME as a primary entry route. The protein corona—particularly ApoE adsorption—critically governs CME by engaging low-density lipoprotein receptors (LDLr) for clathrin- and caveola-mediated internalization[85-88]. Moderna found that the expression of mRNA-LNPs was almost wholly lost in ApoE knockout mice and LDLr knockout mice[62], confirming the importance of protein corona for mRNA-LNP cell uptake.

Macropinocytosis is a form of non-specific cellular uptake of the extracellular fluid and solutes through plasma membrane ruffling. LNPs can also enter cells in this way[27,71]. Reducing pathway-associated regulators or adding inhibitors can reduce LNP cellular uptake by more than 60%[27]. The study inferred that macropinocytosis is induced following CME and seems to be the primary delivery mechanism of LNP in terms of quantity. Interestingly, LNPs themselves appear to induce cellular macropinocytosis[27].

5.2. *Endosomal escape efficiency and kinetics*

Once internalized *via* endocytic pathways, mRNA-LNPs are encapsulated within a membrane-lined vesicle, fusing with the early endosomes. As the endosome matures, the mRNA-LNPs may face three primary fates: escape into the cytosol, degradation in lysosomes following trafficking through late endosomes, or exocytosis back to the extracellular space *via* the recycling endosome pathway (Fig. 5)[89,90]. Critically, functional translation necessitates mRNA localization to the cytoplasm for ribosomal engagement. Therefore, endosomal escape efficiency is the critical determinant of mRNA-LNP delivery efficacy. One study indicated that less than 2% of siRNA underwent endosomal escape[27]. Sabines et al.[62] utilized fluorescence *in situ* hybridization to quantify cytosolic mRNA delivery, measuring an escape efficiency of 2.5% for MC3-based LNPs. Furthermore, the team investigated a novel lipid (Lipid 5, systematically named heptadecan-9-yl 8-((2-hydroxyethyl) (8-(nonyloxy)-8-oxooctyl)amino)octanoate), which significantly enhanced escape efficiency to 15%[62]. This improvement was correlated with markedly increased protein expression *in vivo*. A key mechanistic insight is that increased fusogenicity drives the enhanced efficacy.

The primary site of LNP endosomal escape remains debated, with evidence supporting distinct compartments such as early endosomes, recycling tubules, or early-late hybrid endocytic compartment[27,91,92]. Patel et al.[93] observed that late endosome/lysosome formation is crucial for the efficient delivery of exogenous mRNA. As for the kinetics, Wittrup et al.[94] found that endosomal release of siRNA occurred within ∼5−15 min of endocytosis. Besides, internalized mRNA-LNPs can also produce specialized extracellular vesicles (EVs). Maugeri et al.[95] discovered that a fraction of hEPO mRNA and ionizable lipids from hEPO-mRNA-LNPs—specifically, components that neither dissociate/escape into the cytosol nor undergo degradation within endosomes—can be packaged into endosomally derived extracellular vesicles (endo-EVs) and secreted extracellularly. In contrast to administered mRNA-LNPs, the molar ratio of mRNA to ionizable lipid in endo-EVs is 1:1. Interestingly, intravenous administration of endo-EVs led to detectable plasma hEPO, demonstrating their capacity to deliver functional mRNA and mediate protein expression *in vivo*.

6. Plasma pharmacokinetics, metabolism, and excretion of mRNA-LNPs

Preventive mRNA vaccines are typically administered *via* IM injection[96,97], functioning by encoding antigenic proteins that leverage the immune system's inherent amplification pathways to mount robust immune responses. However, the resulting efficacy and its duration are not directly proportional to the level or persistence of the antigen expression. Other mRNA applications—such as cancer vaccines, gene editing therapies, and autoimmune disease treatments—can access a wider array of administration routes (Table 1)[98], such as intratumoral, intravenous and inhaled delivery. Compared with preventive mRNA vaccines, the plasma pharmacokinetic (PK) profile of IV-administered mRNA therapeutics is critical for predicting effective dosing and regimens[99]. Additionally, unlike established helper lipids (*e.g.*, cholesterol and DSPC), the biodegradability of novel LNP excipients—such as ionizable lipids and PEG-lipids—correlated with tissue clearance, injection-site inflammation, and safety profiles[100,101]. A comprehensive pharmacokinetic characterization of these excipients is essential for assessing biocompatibility and the risk of adverse reactions. Since biodistribution has been separately discussed in Section 3 ("Biodistribution of mRNA-LNPs"), this section will focus on plasma pharmacokinetics, metabolism, and excretion.

6.1. *Plasma pharmacokinetics*

mRNA-1944 comprises two mRNAs encoding the heavy and light chains of CHKV-24 IgG, delivered *via* LNP-encapsulated intravenous infusion, to enable *in vivo* expression of functional neutralizing antibodies. Its mRNA component exhibits a distinctive PK profile: an initial sharp decline, succeeded by an extended terminal phase[102]. Similar plasma PK profiles were also observed for the mRNA components of mRNA-3927, mRNA-3705, and mRNA-3210[18]. This trend may vary across different species and dosing levels[21]. Notably, the half-life of mRNA in mRNA-1944 (∼80 h) is significantly longer than that of its ionizable lipid component (∼7 h)[102], This phenomenon may be attributed to the rapid metabolism of the ionizable lipid and/or the possibility that

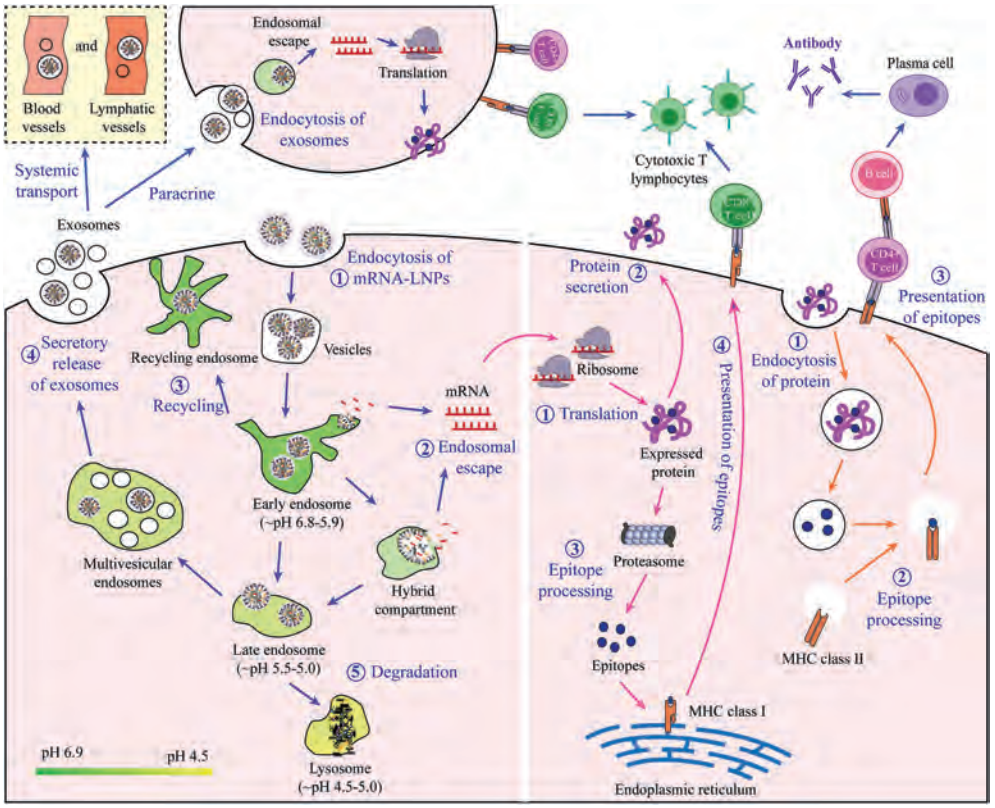

Figure 5 Following cellular uptake of mRNA-LNPs, acidification of endosomes triggers four distinct trajectories (blue arrows): ③recycling to the cell membrane *via* endosomal trafficking for extracellular release; ④packaging into exosomes through multivesicular body processing; ⑤degradation by lysosomal enzymes; or ②endosomal escape (the critical step for protein expression). Ribosomes translate escaped mRNA into antigenic proteins, which activate two immune pathways: 1) endogenous presentation (pink arrow): proteasomal processing generates peptides that are loaded onto major histocompatibility complex class I (MHC class I) molecules, activating $CD8^+$ cytotoxic T cells; 2) exogenous presentation (orange arrow): secreted proteins are internalized by APCs, processed into peptides, and loaded onto MHC class II molecules for $CD4^+$ T cell activation. These cells mediate downstream immunity by inducing B cell maturation into plasma cells.

the detected mRNA is primarily encapsulated within other carriers, such as exosomes.

In preclinical pharmacokinetic studies of the Pfizer/BioNTech COVID-19 vaccine, Wistar Han rats were intravenously administered luciferase-encoding mRNA-LNPs (1 mg/kg), corresponding to 15.3 and 1.96 mg/kg for ALC0315 and ALC0159, respectively. They both exhibited distinct biphasic elimination kinetics. The initial rapid clearance phase showed half-lives of 1.62 h (ALC0315) and 1.72 h (ALC0159), followed by a prolonged terminal elimination phase with half-lives of 139 and 72.7 h, respectively[57]. This aligns with the plasma PK profile of DLin-MC3-DMA (ionizable lipid) in Patisiran. Furthermore, DLin-MC3-DMA also exhibits a longer terminal half-life than PEG2000-C-DMG (PEG-lipid)[103]. The study hypothesizes that the initial rapid clearance may stem from prompt shedding of PEG-lipids post-dose, which facilitates hepatocyte uptake of LNPs *via* the ApoE-dependent LDLr pathway. The prolonged terminal half-life of the ionizable lipid, however, may originate from the subsequent exocytosis of the nucleic acid-lipid complex back into the systemic circulation.

6.2. *Metabolism*

Ionizable/PEGylated lipids exhibit biodegradability *via* metabolic elimination. Pfizer/BioNTech assessed metabolism across species (mouse, rat, monkey, human) using *in vitro* (liver microsomes, hepatocytes, S9 fraction) and *in vivo* (PK study samples of rat) models. ALC0315 undergoes sequential ester hydrolysis: monoester → doubly deesterified metabolite → glucuronide conjugate (exclusively in rat urine). Hydrolysis also yields 2-hexyldecanoic acid (Fig. 6)[104]. Besides, ionizable lipids may undergo β-oxidation. A study revealed the *in vivo* metabolism of [^{14}C]-labeled lipid 5 in rats following a single intravenous administration of mRNA-LNP[105]. At 1 h post-dosing, plasma contained intact lipid 5 and diacid ester hydrolytic metabolites. As time progressed, lipid 5 was cleared from plasma, with the only detected [^{14}C]-labeled lipid 5 metabolites being the diacid with a four-carbon chain-length reduction in both chain linkers. Intact [^{14}C] lipid 5 was barely detectable in urine and feces, which were dominated by diacid metabolites. ALC0159 metabolism involves amide bond hydrolysis, producing *N*, *N*-ditetradecylamine and PEG[104].

6.3. *Excretion of ionizable/PEGylated lipids*

Following IV administration of luciferase-encoding mRNA-LNPs (1 mg/kg) to rats, neither ALC0315 nor ALC0159 was detected in urine, while their fecal elimination profiles demonstrated distinct characteristics: approximately 1% of ALC0315 and 50% of ALC0159 were eliminated through feces in their original molecular forms[104]. Given the minimal detection of unmodified ALC0315 in both urinary and fecal outputs, metabolic

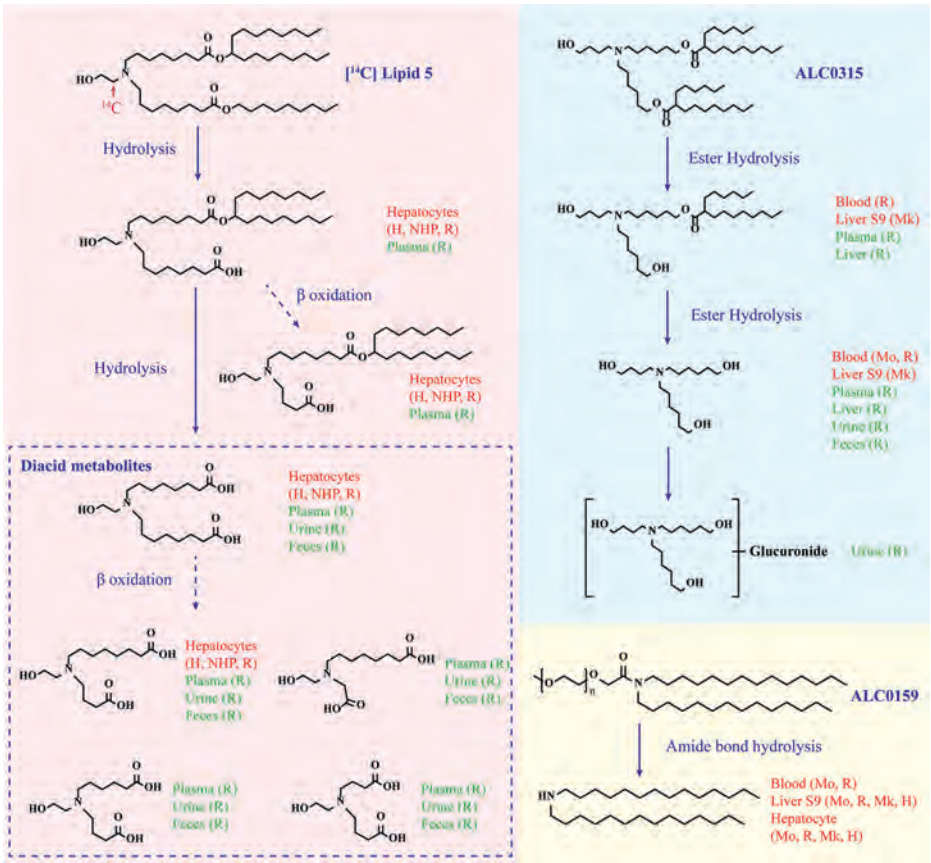

Figure 6 Metabolic pathways of [^{14}C] lipid 5, ALC0315, and ALC0159. The identified metabolites may originate from *in vitro* incubation (red) and/or *in vivo* studies (green). The species abbreviations used in the figure are as follows: H, human; R, rat; Mo, mouse; and Mk, monkey. Reprinted with permission from Burdette et al.[105] Copyright © 2023, under a Creative Commons CC-BY license. The other data was sourced from (125742_S1_M2_24_nonclinical-overview.pdf (phmpt.org)).

transformation appears to constitute the predominant elimination pathway for this compound. However, the excretion patterns of its metabolites remain unquantified.

7. Research toolkits

Studying the biodistribution and pharmacokinetics of LNPs is critical to assessing their targeting efficiency, therapeutic efficacy, and safety profiles. Various analytical methods can be employed based on the analytes or experimental objectives, including radiolabeling, fluorescence/bioluminescence imaging, mass spectrometry-based assays, and hybridization techniques. For example, hybridization probes are optimal for mRNA quantification due to their exceptional sensitivity, whereas fluorescent or radiolabeling techniques are superior for dynamic *in vivo* tracking. In this section, we discuss the strengths and weaknesses of these methods for investigating the *in vivo* fate of mRNA-LNPs.

7.1. Radiolabel-based technologies

Radiolabel-based technologies enable high-sensitivity detection of radionuclides in biological tissues, providing spatially resolved distribution maps. Key technologies for biodistribution studies include quantitative whole-body autoradiography (QWBA), positron emission tomography (PET), and single-photon emission computed tomography[106,107]. Among these, QWBA is routinely applied in preclinical biodistribution assessments of nucleic acid therapeutics[108-110]. Preclinical QWBA studies typically utilize albino and pigmented rats. Data from albino rats correlate with toxicity profiles, whereas data from pigmented rats predict human radiation exposure due to melanin-binding-induced radiolabel accumulation[111]. QWBA preserves native tissue architecture with minimal disruption, enabling accurate *in situ* biodistribution profiling while mitigating cross-contamination risks. However, it also exhibits certain limitations. Firstly, this technique typically requires processing into tissue sections for monitoring, which is not conducive to dynamic assessment. In contrast, PET-CT excels in dynamic real-time monitoring, capturing tracer kinetics critically for characterizing particle translocation dynamics[112]. For instance, Lindsay et al.[113] used a radionuclide-near-infrared dual-probe to label mRNA. They monitored the dynamic drainage signals of the mRNA vaccine from muscle to lymph nodes *via* positron emission tomography-computed tomography and near-infrared imaging technologies. Secondly, QWBA cannot distinguish between the drug (carrier or material) and its metabolites. Several studies have found that the broad biodistribution observed using QWBA is often attributable to degradation products or metabolites, especially when applying less stable isotopic labeling in used (*e.g.*, ^{3}H, ^{125}I)[111]. One study demonstrated that ^{3}H-labeled siRNA lost 9% of the label after 2 h and 26% after 48 h post-IV injection[114]. This underscores the importance of evaluating

radiolabel stability and accounting for the effects of analyte metabolism during the research. Furthermore, QWBA tissue sections typically require dehydration, which may lead to the loss of volatile metabolites. Mass spectrometry imaging technology offers a promising alternative for addressing these issues of metabolite loss and distribution distortion. For cell-targeting LNPs, achieving cellular-level resolution is considered essential. However, QWBA lacks cellular resolution due to freezing-induced morphological disruption. Consequently, microautoradiography serves as the preferred method for analyzing drug distribution at the cellular level[110].

7.2. Mass spectrometry

Mass spectrometry (MS) achieves analyte identification by measuring mass-to-charge ratios and enables precise compound characterization when integrated with separation techniques. To date, MS-based methodologies have been well-established for pharmacokinetic profiling of lipid components and metabolite identification[108,109,115], exemplified by Pfizer/BioNTech's studies on lipid pharmacokinetics[57] and Moderna's screening for optimized LNP formulations[56]. For tissue distribution studies, conventional homogenization methods provide quantitative data but fail to reveal the spatial localization of analytes within tissues. In contrast, MSI enables spatially resolved lipid distribution analysis in intact tissues[116-118]. For example, Christensen et al.[109] successfully mapped the biodistribution of the lipid DLin-KC2-DMA using matrix-assisted laser desorption ionization mass spectrometry imaging.

Despite these advances in lipid analysis, direct MS characterization of mRNA faces critical challenges. Macromolecular mRNA (10^5−10^6 Da) sometimes exceeds the detection range of conventional MS[119]. Lowenthal et al.[120] recently established an acid hydrolysis-isotope dilution MS technique for the quantification of LNP-encapsulated mRNA in formulated products. Acid hydrolysis simultaneously releases mRNA cargo from LNPs and hydrolyzes it into constituent nucleobases for quantification. Although this method ensures accuracy, its sensitivity remains lower than that of conventional polymerase chain reaction (PCR). More importantly, it does not resolve key challenges such as *in vivo* mRNA quantification or the distinction between complex mRNA forms (intact *vs.* degraded, free *vs.* encapsulated). Beyond nucleic acids, MS platforms also support characterization of vaccine-associated proteins, including antigen proteins and corona proteins, among others[121,122].

7.3. Fluorescence imaging

Fluorescence imaging (FLI) and BLI enable non-invasive tracking of mRNA-LNP biodistribution. Their core distinction lies in the emission mechanism; FLI requires excitation by light of specific wavelengths to stimulate fluorescent dyes or proteins, enabling detection of their emitted light. In contrast, BLI typically involves the administration of luciferase-encoding mRNA-LNPs, followed by the injection of the corresponding substrate (*e.g.*, luciferin) to initiate an enzymatic reaction that emits light. Both techniques are extensively applied to track the spatial and temporal distribution of mRNA-LNP formulations in preclinical models.

LNPs can be labeled with lipophilic dyes (*e.g.*, DiD, DiR, DiO) for *in vivo* imaging[58,123,124]. However, these dyes can potentially modify the physicochemical properties of the entities being labeled. Moreover, one study demonstrated that the dye ICG leaks from LNPs after intravenous administration, impairing the characterization of biodistribution. This leakage likely relates to its amphiphilic properties and localization within LNPs, underscoring the need for prudent selection of suitable fluorescent dyes[125]. For mRNA tracking, dyes such as Cy5 and Cy7 enable tracing but introduce steric hindrance and hydrophobicity, impairing transcription and translation[126]. Alternative techniques—including nanocarrier-conjugated probes (*e.g.*, gold nanoparticles) and aptamer fusion strategies—also compromise translation efficiency or disrupt RNA-protein interactions[127,128]. In contrast, chemical modification approaches (*e.g.*, azide-functionalized 5′-cap analogs or 3′-polyA tails) exhibit minimal interference and enable post-transcriptional labeling in cells, though limited labeling sites result in low signal intensity[129,130]. Baladi et al.[126] developed a fluorescent tricyclic cytosine analogue that not only generates sufficient fluorescence for visualization but critically maintains translational competence, showing promise for mRNA-LNP delivery studies. Furthermore, LNP formulations encapsulating mRNA, which encodes fluorescent proteins, are commonly employed to investigate the biodistribution of mRNA-LNPs[61,115].

BLI leverages luciferase-substrate reactions to generate bioluminescent signals, enabling non-invasive tracking of luciferase proteins[131,132]. BLI eliminates the problem of autofluorescence, thereby providing superior specificity compared to FLI. Combining numerous imaging modalities often provides richer dynamic information. For instance, Ma et al.[133] utilized DiR-labeled LNPs encapsulating Cy5-labeled luciferase mRNA to track real-time biodistribution *via* FLI and BLI. By leveraging the fluorescence resonance energy transfer (FRET) between Cy5 and DiR, they monitored mRNA dissociation from LNPs through the recovery of Cy5 fluorescence signals. Additionally, transgenic models such as Ai14 mice enable indirect assessment of functional mRNA delivery and expression. In this system, the delivery of Cre-encoding mRNA-LNPs leads to the translation of Cre protein, which catalyzes the excision of a genomically integrated lox*P*-Stop-lox*P* cassette, thereby activating tdTomato fluorescence expression as a readout[72,88].

In mRNA vaccine research, luciferase-encoding mRNA is frequently employed as a surrogate to indirectly infer the biodistribution of mRNA-LNPs, as LNPs are widely regarded as the dominant factor governing biodistribution. However, the signal reflects protein expression rather than LNP distribution. Furthermore, the intrinsic kinetics of luciferase should be carefully considered, as significant discrepancies in biodistribution patterns may arise between luciferase and the functional protein. For instance, luciferase is a short-lived protein with a half-life of approximately 2 h in living HEK293 cells[134], whereas SARS-CoV-2 spike protein exhibits substantially longer persistence (>8 h in BEAS-2B cells)[135]. Notably, for mRNA therapeutic drugs, the expression level and duration of the encoded protein in target tissues influence the onset and duration of drug efficacy. This suggests that surrogate methods used to study mRNA vaccines' biodistribution may not apply to mRNA therapeutics.

7.4. Hybridization techniques

ISH is a fundamental molecular technique for visualizing specific nucleic acid sequences (DNA or RNA) through complementary probe hybridization, allowing for precise spatial localization within biological samples[136-138]. Fluorescence *in situ* hybridization (FISH) is the gold standard for RNA detection in fixed specimens, offering unparalleled specificity and resolution[139,140].

Moderna utilized single-molecule FISH to quantify the intracellular delivery of mRNA therapeutics[62]. bDNA technology employs sequential sandwich hybridization and branched DNA-mediated signal amplification (rather than target amplification) to generate a chemiluminescent signal directly proportional to the original nucleic acid amount, providing a highly sensitive method for quantifying low-abundance targets such as *in vivo* mRNA[60,62,141]. For instance, Moderna utilized bDNA to quantify six encapsulated mRNA species in various tissues during preclinical evaluations, underscoring its capacity for multiplexed analysis[142]. Other techniques, such as quantitative reverse transcription PCR, RNAscope, and nucleic acid sequence-based amplification, droplet digital PCR, provide complementary strategies for mRNA detection and quantification[143-146].

Besides, hybridization-based methods enable evaluation of endosomal escape efficiency when used in conjunction with FRET technology. Zhang et al.[147] developed a Cy5/BHQ3-labeled partially complementary double-stranded DNA probe targeting *GAPDH* mRNA. In its double-stranded state, Cy5 fluorescence is quenched by BHQ3 *via* FRET. Upon delivery into the cytoplasm, the BHQ3-labeled single-strand DNA in the probe is competitively displaced by *GAPDH* mRNA, leading to Cy5 fluorescence recovery detectable by a confocal laser scanning microscope. This probe serves as an indirect indicator of cargo accessibility and delivery system efficiency—rather than direct mRNA release dynamics—while overcoming limitations of conventional mRNA labeling.

ISH technology is primarily employed for the spatial distribution mapping and quantification of nucleic acids within tissues or cells. However, it is unsuitable for *in vivo* dynamic tracking due to its requirement for tissue fixation, along with limitations in probe stability and spatial resolution[126]. Additionally, due to the length limitations of RNA probes, this method may be unable to distinguish whether detected signals originate from intact mRNA or degradation fragments, which could compromise the establishment of a correlation with protein expression. By employing a combination of probes targeting multiple regions, it is possible to assess the integrity of the target mRNA.

7.5. ELISA

The enzyme-linked immunosorbent assay (ELISA) represents a fundamental technique for the quantitative analysis of a broad spectrum of analytes, including proteins, hormones, antibodies, and immune markers, through four primary formats: direct, indirect, sandwich, and competitive ELISA[148,149]. It serves as a comprehensive tool in mRNA-LNP vaccine development, enabling precise antigen quantification (*e.g.*, receptor-binding domain)[150], antibody profiling[151-153], monitoring of cytokine dynamics[154], and safety assessment by detecting PEG-specific antibodies[155], thereby providing critical insights into vaccine-induced humoral immunity, immune polarization, and potential hypersensitivity reactions. ELISA provides exceptional sensitivity (enabling picogram-level detection), high-throughput capacity, and enhanced safety. Nonetheless, it remains prone to cross-reactivity artifacts caused by nonspecific antibody binding, which can undermine assay specificity and generate false-positive or false-negative signals.

7.6. Barcoding technologies

DNA barcoding represents a novel high-throughput screening technique for *in vivo* LNP analysis. Each LNP is formulated with nucleic acids containing a unique barcode sequence, enabling the tracking of nanoparticle delivery by sequencing these barcodes in target cells or tissues. For example, Huayamares et al.[156] evaluated 94 LNP formulations using DNA barcoding combined with PCR technology, identifying delivery systems capable of targeting head and neck squamous cell carcinoma. While DNA barcoding enables high-throughput screening, it does not directly report mRNA translation levels. Co-delivering mRNA with DNA barcodes resolves this limitation by providing concurrent protein expression data, thereby enabling the identification of LNPs with optimal delivery and functional efficacy. Sanchez et al.[157] exemplified this approach by screening 128 LNP formulations co-delivering *Cre* mRNA and DNA barcodes, which enabled the simultaneous evaluation of biodistribution and functionality. Liu et al.[146] systematically assessed the biodistribution and delivery efficacy of mRNA-LNPs in mice by integrating dsDNA barcoding with qPCR and BLI.

Beyond DNA-based barcoding strategies, several novel barcode approaches have demonstrated promising screening efficacy. For instance, Rhym et al.[158] developed a LC−MS/MS method to detect peptide barcodes translated from mRNA, enabling the evaluation of 384 structurally distinct ionizable lipids *in vivo*. Separately, Wang et al.[159] created Quantitative Analysis of Reverse Transcribed Barcodes, which employs a bacterial retron reverse transcription system to couple the cytoplasmic delivery of functional mRNA with the readout of cDNA barcodes.

In summary, monitoring only a single component within mRNA-LNP cannot effectively confirm their successful delivery and functional activity in target cells. Multimodal analytical approaches are therefore essential for comprehensive characterization of mRNA-LNP pharmacokinetics and biological fate. The integrated use of traditional molecular probes (fluorescence/bioluminescence), radiolabeling, and novel barcoding strategies provides a transformative platform for rapid screening of tissue-specific LNP with high delivery efficacy.

8. Enhancing the efficacy, targeting, and safety of mRNA-LNPs

LNPs have shown remarkable efficacy in delivering RNA therapeutics, yet they still require further optimization in terms of delivery efficiency, targeting specificity, safety, and immunogenicity. This section will address these key challenges to facilitate the design optimization of next-generation LNPs and broaden the scope of mRNA-LNP applications.

8.1. Enhancing the efficacy of mRNA-LNPs

8.1.1. Enhancing the delivery efficiency of LNP by optimizing lipid design and composition

Enhancing endosomal escape efficiency is critical for improving protein expression. Refining LNP design and formulation serves as the central focus for boosting endosomal escape, with ionizable lipid optimization currently representing the most extensively researched approach. Ionizable lipids have three structural components: the headgroup, linker, and tail. Variations in lipid architecture—such as the number of headgroups, the unsaturation degree and hydrophobicity of tails, the position and conformation of unsaturated bonds, and the quantity and length of tails—significantly influence the delivery efficiency of LNPs[160-162]. For instance, incorporating a trialkyl lipid into LNPs

promotes adoption of the reversed hexagonal phase, which enhances disruption of the endosomal membrane[61]. Lam et al.[61] developed and screened a range of trialkyl ionizable lipids, identifying the optimal candidate (Lipid 10). Lipid 10-based LNPs demonstrated stronger gene silencing capability and improved tolerability than those of MC3-based LNPs. Further comparative studies on ionizable lipids with 2, 3, and 4 tails—all featuring an imidazole headgroup—revealed that the 4-tailed variants achieved the most efficacious outcomes[163]. Mrksich et al.[164] engineered a combinatorial library of ionizable lipids with variable tail lengths. Compared to the benchmark C12-200, LNPs formulated with C10-200 (shorter-tail IL) enhanced liver transfection of luciferase mRNA (1929 bp) by over 10-fold. For *Cas9* mRNA (4521 bp), C9-200-based LNPs elicited over threefold the number of insertion/deletion relative to C12-200 controls. This suggests that the optimal lipid tail lengths differ for mRNA of different sizes, indicating that the structure and proportions of ionizable lipids may still require further optimization for mRNA drugs intended for distinct therapeutic purposes.

The linker, typically composed of ether, ester, or amide bonds that connect the headgroup and tail, also influences delivery efficiency. For instance, when the cross-section area of the hydrophobic tail exceeds that of the hydrophilic head, LNPs tend to adopt a cone-shaped morphology, facilitating endosomal escape and improving delivery efficiency[165]. Leveraging this feature, Liu et al. designed ionizable lipids with branched β-isobutylglutarate linkers, enhancing LNP transfection efficacy. Separately, Chen et al. developed GSH-responsive degradable lipids featuring disulfide-bridged ester linkers, whose conical structure promoted exceptional endosomal escape and swift mRNA release kinetics[166].

An intriguing study revealed that the stereochemistry of ionizable lipids significantly impacts delivery efficiency and tolerability. Specifically, C12-200-S-based LNPs achieved higher mRNA delivery levels than their racemic and C12-200-*R* counterparts, respectively[157]. Notably, stereopure LNPs demonstrated superior *in vivo* tolerability compared to racemic formulations. However, another study suggests that the influence of ionizable lipid stereochemistry on delivery outcomes may vary across different molecular systems[167], underscoring the critical need to elucidate how chemical structure governs LNP activity and tolerability profiles.

Modifications to lipid components represent an effective strategy for enhancing mRNA delivery efficiency. One study incorporated a novel fluorinated ionizable lipid (F-L319) into L319-based LNPs, the resulting LNPs significantly outperformed L319-LNPs or F-L319-LNPs alone in *in vivo* mRNA delivery efficiency[168]. Separately, asymmetric sterol-conjugated ionizable lipids were engineered to enable prolonged and safe mRNA delivery[169]. In addition, modifying helper lipids such as cholesterol can also modulate endosomal escape. Studies demonstrated that substitution of conventional cholesterol with the ionizable cholesterol analog 3β[L-histidinamide-carbamoyl] cholesterol markedly enhanced GFP expression[170]. This improvement is likely due to protonation of the histidine imidazole group in the novel cholesterol analog within endosomes, which promotes endosomal escape. Similarly, Patel et al.[171] identified β-sitosterol-based LNPs that exhibit superior transfection efficiency, likely due to their polyhedral morphology. Notably, while these novel ionizable lipids demonstrate superior protein expression efficiency, current studies lack comprehensive characterization of their *in vivo* immunogenicity, biodegradability, and targeting specificity. Hence, these advanced materials warrant further investigation. Moreover, pronounced species differences compel therapeutic validation in large-animal models, notably NHPs, to confirm clinical efficacy.

Incorporating a fifth component into conventional LNPs serves as an additional strategy to enhance mRNA delivery efficiency. For instance, Bogaert et al. strategically enhanced cytosolic delivery of siRNA and mRNA in LNPs by partially replacing cholesterol with cationic amphiphilic drugs, a class of compounds proven to facilitate intracellular transport of small nucleic acids[172]. The integration of tetraether lipid caldarchaeol (an archaeal ether lipid) into LNPs significantly enhanced delivery efficacy, demonstrating up to a 10-fold increase *in vitro* mRNA expression, potentially attributed to this lipid's fusogenic and lyotropic properties[173]. Besides, incorporation of membrane-intercalating conjugated oligoelectrolytes COE-S6 into mRNA-LNPs increased systemic luciferase expression by 1.75-fold post intravenous injection[174]. Furthermore, introducing negatively charged polymers into LNPs is another feasible method to enhance mRNA delivery efficiency by facilitating the diffusion and dissociation of the mRNA from its carrier. Zhang et al.[147] enhanced cytoplasmic mRNA release by incorporating poly(γ-glutamic acid) into mRNA-LNPs. Subsequent *in vivo* studies confirmed that optimized mRNA-LNP formulations achieved 5- and 3-fold increases in luciferase expression following IV or IM administration, respectively.

Low endosomal escape efficiency can also be addressed by altering cellular uptake mechanisms or intracellular trafficking pathways. For instance, a study demonstrated that pretreating cells with a complementary lipopeptide and using coiled-coil peptide-modified LNPs enabled substantial genetic cargo delivery by bypassing endocytic pathways. This approach yielded up to a 63-fold increase in GFP expression *versus* that of unmodified LNPs[175]. However, it should be noted that this efficient delivery can only be achieved through cell pretreatment and thus may hold potential applications in adoptive cell therapy. Wang et al.[176] developed a noncationic thiourea-based LNP system that evades intracellular recycling pathways, a common mechanism that expels internalized nanoparticles to the extracellular space. By inhibiting this efflux, the system substantially boosted gene transfection efficiency.

8.1.2. Improving the immunogenicity of preventive vaccines

The primary function of preventive vaccines is to establish long-term protective immunity by eliciting immune responses. Engineering adjuvant functionality into LNPs enables synergistic enhancement of innate immune activation and antigen-specific adaptive responses. Han et al.[177] engineered an adjuvant lipidoid that enhanced mRNA delivery and conferred TLR7/8-agonism *via* partial substitution in LNPs, boosting SARS-CoV-2 vaccine innate immunity in mice. Misra et al.[178] developed LNPs co-encapsulating the TLR7-selective adjuvant CL347, doubling IFN-γ^+ $CD4^+$/$CD8^+$ T cells in lymphoid organs *versus* non-adjuvanted controls. While mRNA vaccines effectively induce adaptive immune, their protection is often short-lived. Enhancing longevity of immune memory remains a critical challenge[179]. Microbiota-derived metabolites represent promising adjuvant candidates to enhance $CD8^+$ T cell memory[180,181]. By incorporating microbiome metabolites (*e.g.* butyrate) into LNPs, one study achieved enhanced generation of stem cell-like memory T cells and amplified memory T cell responses, indicating a promising strategy for durable immunity[179].

8.1.3. Enhancing the efficacy of therapeutic applications

To enhance therapeutic efficacy, innovative LNP strategies are being developed to overcome biological barriers by co-delivering

synergistic therapeutic agents. Li et al.[182] demonstrated that dexamethasone pretreatment enhanced the luciferase expression in mice and monkeys. Mechanistic studies revealed that dexamethasone inhibited the phagocytosis by macrophages, thereby increasing the accumulation of LNPs in hepatocytes. This strategy consequently enhanced the efficacy of protein replacement and genome editing therapies. In another study, Park et al.[183] engineered an LNP co-delivery system for *IL*-12 mRNA and indoximod prodrug. Indoximod inhibits the indoleamine 2,3-dioxygenase pathway, thereby suppressing IL-12-induced activation of immunosuppressive $CD4^+Foxp3^+$ T regulatory cells. This strategy enhanced the effector function of $CD8^+$ T cells and delayed tumor growth, demonstrating a promising approach to cancer immunotherapy. Additionally, emerging research reveals that tumor-derived small extracellular vesicles hijack therapeutic nanoparticles to liver Kupffer cells for degradation, compromising antitumor efficacy. Gong et al.[184] created an LNP co-delivery platform incorporating both mRNA and *Rab27a* siRNA; by suppressing the secretion of tumor-derived small extracellular vesicles, this strategy significantly enhanced therapeutic efficacy, highlighting its potential for oncology applications.

8.2. *Enhancing the targeting of mRNA-LNPs*

8.2.1. *Enhancing the tissue targeting of mRNA-LNPs*

To broaden the applications of LNPs in diverse RNA therapeutics, developing strategies for effectively targeting specific organs and tissues *in vivo* is imperative. Such advancements would enhance therapeutic efficacy while minimizing adverse effects. Rational design of ionizable lipids serves as a pivotal strategy in current research to engineer LNP targeting specificity, particularly towards spleen and lungs. For spleen targeting, dendron-like ionizable lipids[185], ketal-ester ionizable lipids[167], and carbonate-bearing ionizable lipids[186] effectively mediate delivery. Conversely, ionizable lipids including those with amide bonds in tails[122], piperazine-based ionizable lipids (*e.g.*, 244cis)[187] enable lung tropism of LNPs. Notably, the structural class of the linker can also influence the targeting specificity of LNPs[188]. Furthermore, adding a fifth component to LNPs represents a critical strategy for modulating targeting specificity. A prime example is the development of SORT LNPs, where by incorporating SORT lipids into the formulation, their targeting profile was altered, thereby enabling efficient delivery to multiple organs and cell types, including the lungs, spleen, epithelial cells, and immune cells[72,189]. Liu et al.[190] synthesized several ionizable cholesterol analogs as a fifth LNP component. Their study demonstrated that after IV injection, the 0315-Ergo-40% formulation resulted in splenic fluorescence accounting for 95% of the total signal across major distribution organs (liver, lungs, and spleen). Conversely, under the 102-Sito-40% formulation, pulmonary fluorescence constituted 78% of the signal in these organs. This confirms the feasibility of modulating organ selectivity by incorporation of ionizable cholesterol analogs.

Beyond LNPs, other types of carriers can mediate extrahepatic targeting[191,192]. For instance, Lin et al.[193] developed phospholipidated and alkylated polymers (PAPs), where single-component PAPs facilitate spleen-specific mRNA delivery. Furthermore, PAPs synergize with various helper lipids to form LNPs, which enable specific mRNA delivery to the lungs and liver, respectively. A study on polymer-lipid hybrid nanoparticles demonstrated that the organotropism of LNPs is dictated by the side chain length of ionizable amino-polyesters, with shorter side chains (C4—C5) diverting particles to the spleen and lungs, and longer chains (C7—C9) show liver delivery[194]. Alternatively, modifying administration routes can redirect LNP targeting. For example, intratracheal administration or nebulization can mediate pulmonary delivery[195-198].

Targeted delivery research for other organs remains relatively limited compared to spleen and lungs. Isaac et al.[199] engineered an endogenous targeting platform by incorporating cholecalciferol as a fifth component into LNPs. This novel system enables intravenous LNP delivery to the pancreas, offering promising potential for the treatment of pancreatic diseases. For bone targeting, bisphosphonate ligand modification represents an effective classical approach[200], studies demonstrate that ionizable lipids chemically modified with bisphosphonate moieties can efficiently deliver LNPs to the bone microenvironment[124,201]. Notably, an interesting study developed an innovative LNP system designed for bone marrow targeting by incorporating covalent-binding lipid moieties (*e.g.*, stearic acid *N*-hydroxysuccinimide ester) as a fifth component. The underlying targeting mechanism is driven by an endogenous process where the covalent lipids enrich ApoE on the LNP surface. These LNPs transfect at least 14 cell types (including hematopoietic stem cells and immune cells), enabling efficient genome editing in bone marrow and demonstrating potential for treating hematologic diseases[202].

8.2.2. *Enhancing the cell targeting of mRNA-LNPs*

Immune and cancer cells are key preventive or therapeutic targets, with numerous studies exploring LNP targeting strategies by optimizing ionizable lipid. Zhao et al.[203] demonstrated that imidazole-containing lipidoid-based LNPs enable efficient mRNA delivery to T lymphocytes. Fenton et al.[204] designed a novel OF-Deg-Lin-based LNP that delivers mRNA to splenic B lymphocytes and induces protein expression. Furthermore, Suzuki et al.[205] revealed that LNPs with 15% DSPC exhibit rigidity, hydrophobicity, and a charge-neutral surface, thereby suppressing ApoE-mediated hepatic uptake while promoting complement receptor-mediated B cell targeting.

Ligand conjugation to the surface of LNPs—including small molecules, aptamers, and peptides—enables targeted mRNA delivery to specific cells[206]. Tang et al.[207] developed a phenylboronic acid-derived LNP that enables targeted delivery of mRNA to sialic acid-overexpressing tumor cells. Zeng et al.[208] engineered mannosylated LNPs, enabling targeted delivery to APCs. Antibody modification on LNPs represents a pivotal strategy for modulating cell targeting specificity. For instance, CD5 antibody-conjugated LNPs enable efficient mRNA delivery to T lymphocytes, driving robust *in vivo* generation of functional CAR T cells[209]. Another study demonstrated that EGFR-targeted LNPs achieved tumor-specific uptake by disseminated ovarian cancer cells[210]. Shi et al.[211] engineered an LNP functionalized with CD117 antibodies that achieves targeted RNA delivery to rodent hematopoietic stem cell following IV injection. Recently, Papp et al.[212] developed a CD47/tLNP platform by modifying antibody-targeted LNPs with CD47. Their results demonstrated that CD47/tLNP reduced phagocytic clearance and enhanced efficiency of cell-specific delivery.

8.3. *Enhancing the safety of mRNA-LNPs*

8.3.1. *Overcoming the effects of anti-PEG antibodies*

Repeated administration of PEGylated LNPs may induce hypersensitivity, necessitating mitigation strategies to enhance the

safety of mRNA-LNPs and broaden their therapeutic applications. The route of administration and dosage may significantly impact anti-lipid nanoparticle antibodies (ALAs) levels, and these parameters are typically selected based on the specific therapeutic goals. A single-particle antibody measurement assay study examined the production of ALAs in female C57BL/6JRj mice after IV, SC, or IM injections of mRNA-LNPs[213]. The results demonstrated that IM injection consistently produced the lowest ALA levels, regardless of dose—whether administered at a high dose (300 μg/kg) or low dose (0.3 μg/kg). In contrast, SC injection generated the highest ALA concentrations in a dose-dependent manner, while IV administration yielded ALA levels that exhibited inverse dose dependency, aligning with prior observations[214]. These findings indicate that the selection of administration routes requires careful consideration.

Formulation design of mRNA-LNP therapeutics enables engineering of immune responses, including anti-PEG IgE/IgM implicated in hypersensitivity reactions[215,216]. Adjusting the acyl chain length of PEG lipids can regulate anti-PEG antibody production. One study compared anti-PEG IgM levels induced by LNPs conjugated to PEG lipids with C14 *versus* C18 acyl chains. The results indicated that LNPs with shorter acyl chain PEG lipids induced lower anti-PEG IgM than those with longer chains. This difference is likely attributable to the enhanced shedding propensity of short-chain PEG lipids from LNPs, whereas free PEG exhibits slight capacity to induce anti-PEG IgM production[217,218]. Additionally, studies have shown that cleavable-branched and branched PEG-lipid derivatives reduce anti-PEG antibody production, mitigating the accelerated blood clearance (ABC) phenomenon[219]. Modifying the surface properties of PEGylated nanoparticles can also fine-tune immune responses. Zhang et al.[220] engineered an anti-PEG single-chain variable fragment, which alleviates the ABC phenomenon by competing with anti-PEG antibodies for binding.

Furthermore, researchers are exploring PEG alternatives—such as poly(*N*-vinylpyrrolidone), polyacrylamides, poly(2-oxazoline)s, and polysarcosine (pSar), as discussed in prior reviews[221-224]. Studies reveal that pSar-formulated LNPs achieve mRNA delivery efficiency comparable to PEG-formulated LNPs with similar *in vivo* safety profiles[225,226]. Critically, pSar-liposomes induce significantly lower IgM/IgG levels than PEG-liposomes, effectively mitigating the ABC phenomenon[227]. Poly(carboxybetaine) lipids (PCB) represent another promising alternative to PEG-lipids. Studies demonstrate that PCB-incorporated LNPs are able to mitigate the ABC effect and exhibit higher endosomal escape efficiency compared with PEG-based LNPs[228]. Recently, Xiao et al.[229] engineered brush-shaped polymer lipids to replace PEG lipids, with novel LNPs demonstrating lower levels of anti-PEG antibody binding and superior therapeutic performance in the field of protein replacement and genome editing, in comparison to DMG-PEG2000-based LNPs.

Appropriate use of immunosuppressants serves as a strategy to mitigate adverse effects. Chen et al.[230] incorporated LD003 (a hydrophobic dexamethasone prodrug) into LNPs encapsulating diverse nucleic acids, effectively reducing immune stimulation. However, the efficacy and broad applicability of immunosuppressants still require further investigation[231]. Besides, clinical screening for pre-existing anti-PEG antibodies is critical to identify individuals at high risk for severe hypersensitivity to PEGylated vaccines[216]. For these patients, alternative modalities—such as viral vector or protein-based vaccines—can be considered after confirming no cross-reactivity to excipients.

8.3.2. Reducing the immunogenicity of ionizable lipids

LNPs may trigger inflammatory responses, leading to vaccine-related adverse reactions such as fever, fatigue, and injection site pain[232]. Research indicates that the potent inflammatory reactions induced by LNPs primarily originate from ionizable lipids[233,234]. A study demonstrated that within ionizable lipids, amine-containing headgroups induce LNP immunogenicity through two key pathways—one is binding to Toll-like receptor 4 and CD1d, and the other is promoting the formation of lipid rafts[235]. Consequently, studies propose replacing ionizable lipids with highly biocompatible alternatives to reduce immunogenicity. For example, researchers developed highly biocompatible, pH-responsive dipeptide-conjugated lipids (DPLs), with a dipeptide (instead of a tertiary amine group) in their lipid headgroups. Optimized DPL-based LNPs achieved anti-OVA antibody production levels on par with SM-102-based LNPs, yet induced significantly lower levels of inflammatory-mediator production[236]. Another study employed trehalose glycolipids to partially replace ionizable lipids, resulting in LNPs that significantly reduced organ toxicity while maintaining gene expression and immunogenicity, confirming the safety enhancement from partial substitution of ionizable lipids[237]. Reducing the proportion of ionizable lipids in LNPs is another strategy to mitigate inflammatory responses. Liu et al.[238] engineered LNPs with 1% mildronate-derived cationic lipid content, achieving mRNA delivery efficiency comparable to SM-102-based LNPs while significantly mitigating inflammation.

8.4. Next-generation mRNA-LNPs

8.4.1. Next-generation LNPs

The broadening scope of RNA therapeutics—encompassing cancer therapy, monogenic diseases and autoimmune diseases—has intensified demand for enhanced delivery platforms. Beyond LNPs, several alternative delivery platforms are being explored, such as EVs[239-245], polymeric nanoparticles[246], and viral vectors[247-249]. Furthermore, hybrid delivery systems exhibit significant versatility, combining the strengths of diverse platforms to address constraints inherent to single-system approaches. For example, one study incorporated fusion-associated small transmembrane (FAST) proteins into LNPs to develop proteolipid vehicles (PLVs). FAST-PLVs, a hybrid system combining viral and non-viral vector features, exhibit extensive tissue distribution and high-efficiency delivery in mouse and NHP models[250].Critically, FAST-PLVs exhibited lower immunogenicity and retained functional activity after repeated dosing. Another study engineered polymer-lipid hybrid nanoparticles boosting 15 kbp pDNA transfection efficiency, advancing large-sized DNA delivery[251].

Hybrid delivery systems have undergone rapid advancement, with extensive documentation of these hybrid systems to date, such as hybrid LNPs[252], EV-based hybrid systems[253-255], lipid-polymer hybrid systems[256-258], nanoparticle-hydrogel hybrid systems[259,260], and hybrid PLGA nanoparticles[261]. Compared with single delivery systems, hybrid systems demonstrate enhanced stability and delivery efficiency, establishing them as promising therapeutic platforms. However, their complex compositions necessitate greater production resources and expertise, while increased structural complexity may heighten regulatory approval barriers.

8.4.2. Next-generation mRNA

mRNAs serve as the functional components of mRNA-based vaccines and therapeutics. Currently, three distinct types of mRNA

are utilized in pharmaceutical development: non-replicating mRNA, self-amplifying mRNA (saRNA), and circular mRNA (circRNA). saRNA vaccines are engineered from the genomes of RNA viruses, mainly alphaviruses[262]. The key advantage lies in self-replication capability, significantly reducing the RNA dose required for vaccination. Merely 10 ng of saRNA induces robust immunogenicity in mice, while only 5 μg suffices for clinical testing[263]. However, saRNA's propensity to trigger excessive innate immune responses remains a challenge[264], which could be partially mitigated through rational engineering of ionizable lipids[265].

Owing to their covalently closed structure, circRNA exhibit significantly extended half-lives compared to linear RNA counterparts. This inherent stability prolongs their shelf life, alleviates stringent storage and transportation requirements, and enhances pharmacokinetic accumulation across diverse cell types and tissues[266-268]. Despite demonstrating superior immunogenicity over linear mRNA vaccines[269], circRNA vaccines face manufacturing complexity. Developing efficient, low-toxicity mRNA therapeutics hinges critically on optimizing production and purification methodologies.

8.5. Enabling clinical adoption of mRNA-LNP therapeutics

Ideal mRNA-LNP candidates require high protein expression, minimal immunogenicity, and long-term safety upon repeated dosing. However, current mRNA-LNPs face challenges that hinder their translation to clinical applications. First, the precise mechanisms governing mRNA-LNP intracellular trafficking, endosomal interactions, and endosomal escape remain incompletely understood. Although strategies such as ionizable lipids designed to disrupt endosomal membranes or inhibition of recycling endosomes have been proposed to enhance escape, elucidating the specific factors controlling this process is critical for advancing delivery efficacy.

Second, in mRNA vaccines, LNPs serve dual roles as carriers and immunostimulatory adjuvants. However, the contribution of LNP-triggered immunity to vaccine adverse reactions remains poorly defined. This adjuvant activity may compromise efficacy in non-vaccine applications, particularly protein replacement therapies, during repeated administration. Consequently, mitigating LNP immunogenicity is a critical research priority. Furthermore, the *in vivo* pharmacokinetics of classic LNP components (ionizable lipids, PEG-lipids, cholesterol, phospholipids) is often overlooked. Given the immunogenic risks of ionizable/PEG-lipids, elucidating their metabolism and elimination pathways is essential for safety optimization.

Third, the optimization of mRNA-LNP delivery systems demands further refinement. Critical aspects include the design, synthesis, and purification of mRNA to enhance translation efficiency and mitigate innate immune activation. However, the efficacy of nucleoside modifications in systemically administered mRNA-LNPs may vary with LNP composition and target organ/cell types[270], necessitating deeper exploration of the relationship among modification strategies, translational output, and tissue/cell specificity.

Fourth, species differences have hindered progress in clinical translation. Although *in vitro* assays provide rapid and cost-effective insights, their predictive reliability for *in vivo* performance remains limited[271]. Bridging the gap between controlled *in vitro* systems and complex *in vivo* physiology remains a significant translational challenge[272]. Historically, LNP compositions have been optimized in rodents due to ethical and economic considerations. However, translating potency data from rodents to NHPs—especially for intravenously administered products—has proven difficult. Key LNP parameters, including particle size and lipid ratios, vary significantly across species[273]. Consequently, preclinical validation of nucleic acid sequences and LNP designs in NHP models is essential. Terminal-use NHP studies may offer a strategy to reduce animal use while generating clinically relevant data[274].

Fifth, significant differences in immune function exist across age groups[275]. Therefore, preclinical studies should establish appropriate models to investigate the impact of age on vaccine efficacy[276]. Adjuvants may be an effective strategy to enhance vaccination in the elderly population[277]. Furthermore, metabolic disorders affect immune responses, as evidenced by attenuated responses in diabetic and obese mice[278]—a finding that underscores the necessity to personalize mRNA-LNP formulations for specific target populations.

Sixth, mRNA molecules exhibit poor stability at ambient temperatures; therefore, mRNA-LNP vaccines necessitate storage and transport under low (−20 °C) or ultra-low (−70 °C) temperatures. Lyophilized formulations demonstrate extended shelf-life at 4 °C and room temperature without compromising immunogenicity[279,280], positioning this technology as a promising next-generation platform for mRNA vaccine development.

9. Conclusions and perspectives

The proven efficacy of mRNA-LNP in prophylactic vaccines, and its emerging potential in oncology/gene editing, underscore its pivotal role in nucleic acid therapeutics; however, its transition to broader biologics faces multifaceted barriers—including safety risks, off-target accumulation, suboptimal endosomal escape, and transient expression—necessitating elucidation of *in vivo* fate (*e.g.*, component pharmacokinetics, metabolite profiles, and protein biodistribution) to guide next-generation designs. The development of marketed mRNA-LNP vaccines disproportionately underestimates the absorption, distribution, metabolism, and excretion processes of intact mRNA-LNP complexes and their components. While this oversight partly stems from technical limitations in analytical methodologies, it primarily relies on the premise that mRNA-LNP formulations have demonstrated acceptable safety profiles in extensive animal studies and current clinical applications, thereby ostensibly obviating the need for detailed pharmacokinetic characterization. This rationale may hold partial validity for conventional mRNA-LNP vaccine applications. However, as mentioned above, mRNA-LNP vaccines differ fundamentally from other mRNA-LNP-based biologics under clinical development in several critical aspects.

While extensive research has characterized the *in vivo* fate of mRNA-LNPs, current understanding predominantly derives from vaccine studies using IM administration. This contrasts with alternative delivery routes—such as subcutaneous, intradermal, intravenous, and intratumoral injections—employed for other biologics. The composition of the protein corona on nanoparticles dynamically shifts as they transit between different biological fluids[281]. Consequently, administration routes and dynamic transport processes can significantly alter corona formation, ultimately influencing biodistribution. Defining the interplay among injection site microenvironment, LNP interfacial properties, corona composition, and tissue tropism is essential for rational engineering of next-generation mRNA-LNPs. However,

elucidating these relationships requires efficient separation and purification methods to effectively distinguish between original LNP, PEG-lipid-shed LNP, protein corona-coated LNP, and mRNA/lipid complexes, followed by detailed characterization of their compositional and structural features. Regrettably, most current studies continue to directly investigate the relationship between the physicochemical properties of LNPs themselves and tissue distribution or protein expression through trial-and-error approaches. This knowledge gap impedes mechanistic understanding, as current empirical approaches directly correlate initial LNP properties with tissue distribution while overlooking intermediate transformation states.

A fundamental distinction between mRNA-LNP vaccines and other mRNA-LNP biologics lies in the relationship between protein expression and therapeutic efficacy. For vaccines, potency rarely exhibits a direct dose-response correlation with antigen protein expression levels. Instead, vaccine efficacy primarily depends on the tissue microenvironment where the protein antigen resides and the efficiency of immune cell uptake and presentation—as evidenced by limited correlation between protein expression and immunogenicity ($r = 0.54$)[56]. Conversely, gene editing and protein replacement therapies rely on the quantity and biological functionality of the expressed proteins. Endosomal escape remains a critical bottleneck for efficient protein expression from mRNA-LNPs. Macropinocytosis demonstrates considerable potential for enhancing cytoplasmic mRNA-LNP delivery through high uptake capacity and efficient endosomal escape. However, escape efficiency is driven by lipid fusogenicity, endosomal maturation[93], and cell-type-specific pH variations[91,282,283], necessitating further investigation into tissue-specific LNP performance.

Besides, analytical limitations and the dynamic complexity of mRNA-LNP interactions with biological systems often restrict researchers to tracking only a single component—such as a specific lipid or encoded protein—when assessing *in vivo* distribution kinetics. However, accumulating evidence reveals divergent *in vivo* fates among individual constituents—lipids, mRNA, and expressed proteins—indicating substantial compositional reorganization during physiological exposure. Therefore, attempts to represent the biodistribution of intact mRNA-LNPs based solely on partial component tracking—without rigorous differentiation of these structurally remodeled assemblies—are fundamentally biased and methodologically flawed.

In summary, expanding clinical applications for mRNA-LNP therapeutics necessitates a comprehensive dissection of their *in vivo* fate processes. Elucidating structure-activity relationships of ionizable lipids, correlating LNP physicochemical properties with tissue tropism, and evaluating efficacy *versus* safety profiles are pivotal research priorities. Breakthroughs will hinge on innovative analytical platforms (including separation, purification, and structural composition analysis), coupled with the continuous accumulation and correlative analysis of extensive data.

Acknowledgments

This work was supported by the National Natural Science Foundation of China (Nos. 82030107 and 82373944).

Author contributions

Conceptualization: Jingkai Gu and Yong Zhang; methodology: Jingkai Gu, Yong Zhang, and Lili Cui; formal analysis: Xin Xu, Jingkai Gu, Yong Zhang, and Lili Cui; writing—original draft: Xin Xu, Lili Cui, and Yong Zhang; writing—review and editing: Yong Zhang, Jingkai Gu, and Lili Cui; supervision: Jingkai Gu and Yong Zhang.

Conflicts of interest

The authors declare no conflicts of interest.

References

1. Thomas SJ, Moreira E, Kitchin N, Absalon J, Gurtman A, Lockhart S, et al. Safety and efficacy of the BNT162b2 mRNA Covid-19 vaccine through 6 months. *N Engl J Med* 2021;**385**: 1761−73.
2. Baden LR, El Sahly HM, Essink B, Kotloff K, Frey S, Novak R, et al. Efficacy and safety of the mRNA-1273 SARS-CoV-2 vaccine. *N Engl J Med* 2021;**384**:403−16.
3. Goswami J, Cardona JF, Hsu DC, Simorellis AK, Wilson L, Dhar R, et al. Safety and immunogenicity of mRNA-1345 RSV vaccine coadministered with an influenza or COVID-19 vaccine in adults aged 50 years or older: an observer-blinded, placebo controlled, randomised, phase 3 trial. *Lancet Infect Dis* 2025;**25**:411−23.
4. Xu K, Lei W, Kang B, Yang H, Wang Y, Lu Y, et al. A novel mRNA vaccine, SYS6006, against SARS-CoV-2. *Front Immunol* 2022;**13**: 1051576.
5. Panther L, Basnet S, Fierro C, Brune D, Leggett R, Peterson J, et al. 2892. Safety and immunogenicity of mRNA-1647, an mRNA-based cytomegalovirus vaccine in healthy adults: results of a phase 2, randomized, observer-blind, placebo-controlled, dose-finding trial. *Open Forum Infect Dis* 2023;**10**. ofad500.2475.
6. Ananworanich J, Lee IT, Ensz D, Carmona L, Schaefers K, Avanesov A, et al. Safety and immunogenicity of mRNA-1010, an investigational seasonal influenza vaccine, in healthy adults: final results from a phase 1/2 randomized trial. *J Infect Dis* 2024;**231**: e113−22.
7. Lee IT, Nachbagauer R, Ensz D, Schwartz H, Carmona L, Schaefers K, et al. Safety and immunogenicity of a phase 1/2 randomized clinical trial of a quadrivalent, mRNA-based seasonal influenza vaccine (mRNA-1010) in healthy adults: interim analysis. *Nat Commun* 2023;**14**:3631.
8. Akingbola A, Adegbesan A, Adegoke K, Idahor C, Mariaria P, Peters F, et al. Comparing moderna's mRNA-1083 and Pfizer's dual-target mRNA vaccines for influenza and COVID-19. *Npj Vaccines* 2025;**10**:105.
9. Bai HR, Yu XL, Gao Y, Li Q, Wen BG, Hu RK. Highly effective mRNA-LNP vaccine against respiratory syncytial virus (RSV) in multiple models. *Vaccines* 2025;**13**:625.
10. Essink B, Chu LRC, Seger W, Barranco E, Le Cam N, Bennett H, et al. The safety and immunogenicity of two Zika virus mRNA vaccine candidates in healthy flavivirus baseline seropositive and seronegative adults: the results of two randomised, placebo-controlled, dose-ranging, phase 1 clinical trials. *Lancet Infect Dis* 2023;**23**:621−33.
11. Bollman B, Nunna N, Bahl K, Hsiao CJ, Bennett H, Butler S, et al. An optimized messenger RNA vaccine candidate protects non-human primates from Zika virus infection. *Npj Vaccines* 2023;**8**:58.
12. Weber JS, Khattak MA, Carlino MS, Meniawy T, Taylor MH, Ansstas G, et al. Individualized neoantigen therapy mRNA-4157 (V940) plus pembrolizumab in resected melanoma: 3-year update from the mRNA-4157-p201 (KEYNOTE-942) trial. *J Clin Oncol* 2024;**42**. Lba9512.
13. Klinghammer K, Saba NF, Castelluci E, Colevas AD, Rutkowski T, Greil R, et al. 155P BNT113+ pembrolizumab as first-line treatment in patients with unresectable recurrent/metastatic HNSCC:

preliminary safety data from AHEAD-MERIT. *Immunooncol Technol* 2022;**16**:100267.
14. Li N, Li N, Wang Y, Cui N, Wang X, Tang Y, et al. Preliminary safety, antitumor activity, and pharmacodynamics of intratumoral ABO2011 (*IL-12* mRNA) in patients with advanced solid tumors. *J Clin Oncol* 2024;**42**:e14583.
15. Le NT. A phase I study to evaluate the safety and tolerability of JCXH-211 (a self-replicating mRNA encoding IL-12) intratumoral injection in patients with malignant solid tumors: results from the phase Ia dose escalation. *J Clin Oncol* 2024;**42**:2539.
16. Geller DE, Crowley C, Froehlich J, Schwabe C, O'Carroll M. WS10.03 inhaled LUNAR@-CFTR mRNA (ARCT-032) is safe and well-tolerated: a phase 1 study. *J Cyst Fibros* 2024;**23**:S19.
17. Rowe SM, Zuckerman JB, Dorgan D, Lascano J, Mccoy K, Jain M, et al. Inhaled mRNA therapy for treatment of cystic fibrosis: interim results of a randomized, double-blind, placebo-controlled phase 1/2 clinical study. *J Cyst Fibros* 2023;**22**:656−64.
18. Baek R, Coughlan K, Jiang L, Liang M, Ci L, Singh H, et al. Characterizing the mechanism of action for mRNA therapeutics for the treatment of propionic acidemia, methylmalonic acidemia, and phenylketonuria. *Nat Commun* 2024;**15**:3804.
19. Coughlan KA, Eybye M, Henderson N, DeAntonis CM, Frassetto A, Hanahoe E, et al. Improved therapeutic efficacy in two mouse models of methylmalonic acidemia (MMA) using a second-generation mRNA therapy. *Mol Genet Metabol* 2024;**143**:108560.
20. Koeberl D, Schulze A, Sondheimer N, Lipshutz GS, Geberhiwot T, Li L, et al. Interim analyses of a first-in-human phase 1/2 mRNA trial for propionic acidaemia. *Nature* 2024;**628**:872−7.
21. Attarwala H, Lumley M, Liang M, Ivaturi V, Senn J. Translational pharmacokinetic/pharmacodynamic model for mRNA-3927, an investigational therapeutic for the treatment of propionic acidemia. *Nucleic Acid Therapeut* 2023;**33**:141−7.
22. A new RSV vaccine (mResvia) for adults ≥60 years old. *Med Lett Drugs Ther* 2024;**66**:166−8.
23. Weber JS, Carlino MS, Khattak A, Meniawy T, Ansstas G, Taylor MH, et al. Individualised neoantigen therapy mRNA-4157 (V940) plus pembrolizumab *versus* pembrolizumab monotherapy in resected melanoma (KEYNOTE-942): a randomised, phase 2b study. *Lancet* 2024;**403**:632−44.
24. Gillmore JD, Gane E, Taubel J, Kao JT, Fontana M, Maitland ML, et al. CRISPR-Cas9 *in vivo* gene editing for transthyretin amyloidosis. *N Engl J Med* 2021;**385**:493−502.
25. Lee RG, Mazzola AM, Braun MC, Platt C, Vafai SB, Kathiresan S, et al. Efficacy and safety of an investigational single-course CRISPR base-editing therapy targeting *PCSK9* in nonhuman primate and mouse models. *Circulation* 2023;**147**:242−53.
26. Vafai SB, Gladding PA, Scott R, Kerr J, Taubel J, Cegla J, et al. Safety and pharmacodynamic effects of VERVE-101. Available from: https://www.vervetx.com/sites/default/files/2023-11/Verve_AHA_2023_LBS_for%20website.pdf.
27. Gilleron J, Querbes W, Zeigerer A, Borodovsky A, Marsico G, Schubert U, et al. Image-based analysis of lipid nanoparticle-mediated siRNA delivery, intracellular trafficking and endosomal escape. *Nat Biotechnol* 2013;**31**:638−46.
28. Huang J, Yuen D, Mintern JD, Johnston APR. Opportunities for innovation: building on the success of lipid nanoparticle vaccines. *Curr Opin Colloid Interface Sci* 2021;**55**:101468.
29. Rohner E, Yang R, Foo KS, Goedel A, Chien KR. Unlocking the promise of mRNA therapeutics. *Nat Biotechnol* 2022;**40**:1586−600.
30. Jackson LA, Anderson EJ, Rouphael NG, Roberts PC, Makhene M, Coler RN, et al. An mRNA vaccine against SARS-CoV-2 - preliminary report. *N Engl J Med* 2020;**383**:1920−31.
31. Walsh EE, Frenck Jr RW, Falsey AR, Kitchin N, Absalon J, Gurtman A, et al. Safety and immunogenicity of two RNA-based Covid-19 vaccine candidates. *N Engl J Med* 2020;**383**:2439−50.
32. Meo SA, Bukhari IA, Akram J, Meo AS, Klonoff DC. COVID-19 vaccines: comparison of biological, pharmacological characteristics and adverse effects of Pfizer/BioNTech and Moderna vaccines. *Eur Rev Med Pharmacol Sci* 2021;**25**:1663−9.
33. Marchese AM, Rousculp M, Macbeth J, Seet BT, Beyhaghi H, Toback S. The novavax heterologous coronavirus disease 2019 booster demonstrates lower reactogenicity than messenger RNA: a targeted review. *J Infect Dis* 2023;**230**:e496−502.
34. Yanez Arteta M, Kjellman T, Bartesaghi S, Wallin S, Wu X, Kvist AJ, et al. Successful reprogramming of cellular protein production through mRNA delivered by functionalized lipid nanoparticles. *Proc Natl Acad Sci U S A* 2018;**115**:E3351−60.
35. Eygeris Y, Gupta M, Kim J, Sahay G. Chemistry of lipid nanoparticles for RNA delivery. *Acc Chem Res* 2022;**55**:2−12.
36. Schoenmaker L, Witzigmann D, Kulkarni JA, Verbeke R, Kersten G, Jiskoot W, et al. mRNA-lipid nanoparticle COVID-19 vaccines: structure and stability. *Int J Pharm* 2021;**601**:120586.
37. Eygeris Y, Patel S, Jozic A, Sahay G. Deconvoluting lipid nanoparticle structure for messenger RNA delivery. *Nano Lett* 2020;**20**:4543−9.
38. Viger-Gravel J, Schantz A, Pinon AC, Rossini AJ, Schantz S, Emsley L. Structure of lipid nanoparticles containing siRNA or mRNA by dynamic nuclear polarization-enhanced NMR spectroscopy. *J Phys Chem B* 2018;**122**:2073−81.
39. Roces CB, Lou GS, Jain N, Abraham S, Thomas A, Halbert GW, et al. Manufacturing considerations for the development of lipid nanoparticles using microfluidics. *Pharmaceutics* 2020;**12**:1095.
40. Prakash S, Kumar S. Fabrication of microchannels: a review. *Proc Inst Mech Eng B* 2015;**229**:1273−88.
41. Maeki M, Uno S, Niwa A, Okada Y, Tokeshi M. Microfluidic technologies and devices for lipid nanoparticle-based RNA delivery. *J Control Release* 2022;**344**:80−96.
42. Hussain M, Binici B, O'Connor L, Perrie Y. Production of mRNA lipid nanoparticles using advanced crossflow micromixing. *J Pharm Pharmacol* 2024;**76**:1572−83.
43. Channon RB, Menger RF, Wang W, Carrão DB, Vallabhuneni S, Kota AK, et al. Design and application of a self-pumping microfluidic staggered herringbone mixer. *Microfluid Nanofluidics* 2021;**25**:31.
44. Shepherd SJ, Issadore D, Mitchell MJ. Microfluidic formulation of nanoparticles for biomedical applications. *Biomaterials* 2021;**274**:120826.
45. Liu Y, Yang G, Hui Y, Ranaweera S, Zhao CX. Microfluidic nanoparticles for drug delivery. *Small* 2022;**18**:e2106580.
46. Hourdel L, Lebaz N, Peral F, Ripoll M, Briançon S, Bensaid F, et al. Overview on LNP-mRNA encapsulation unit operation: mixing technologies, scalability, and influence of formulation & process parameters on physico-chemical characteristics. *Int J Pharm* 2025;**672**:125297.
47. Chen KF, Yang HF, Cai R. Microfluidics for nanomedicine delivery. *ACS Biomater Sci Eng* 2025;**11**:774−83.
48. Shepherd SJ, Warzecha CC, Yadavali S, El-Mayta R, Alameh MG, Wang L, et al. Scalable mRNA and siRNA lipid nanoparticle production using a parallelized microfluidic device. *Nano Lett* 2021;**21**:5671−80.
49. Zhao L, Xu ZY, Li H, Liu L, Chen SY, Peng ZB, et al. A review of confined impinging jet reactor (CIJR) with a perspective of mRNA-LNP vaccine production. *Rev Chem Eng* 2024;**40**:887−916.
50. Eygeris Y, Henderson MI, Curtis AG, Jozic A, Stoddard J, Reynaga R, et al. Preformed vesicle approach to LNP manufacturing enhances retinal mRNA delivery. *Small* 2024;**20**:e2400815.
51. Tanaka H, Sato Y, Nakabayashi T, Tanaka A, Nishio K, Matsumoto C, et al. A post-encapsulation method for the preparation of mRNA-LNPs *via* the nucleic acid-bridged fusion of mRNA-free LNPs. *Nano Lett* 2025;**25**:6445−53.
52. Wang H, Lauwers H, Gontsarik M, Chen Y, Sanders NN, Cheng MHY, et al. Admixing of mRNA with pre-formed lipid nanoparticles containing a slightly-cationic ionizable lipid allows for efficient mRNA transfection *in vitro* and *in vivo*. *Adv Healthcare Mater* 2025;**14**:e2501788.

53. Heshmati N, Chakka LRJ, Zhang Y, Maniruzzaman M. Fabrication of mRNA encapsulated lipid nanoparticles using state of the art SMART-MaGIC technology and transfection *in vitro*. *Sci Rep* 2024; **14**:22714.
54. Sarode A, Patel P, Vargas-Montoya N, Allawzi A, Zhilin-Roth A, Karmakar S, et al. Inhalable dry powder product (DPP) of mRNA lipid nanoparticles (LNPs) for pulmonary delivery. *Drug Deliv Transl Re* 2024;**14**:360−72.
55. Ogawa K, Aikawa O, Tagami T, Ito T, Tahara K, Kawakami S, et al. Stable and inhalable powder formulation of mRNA-LNPs using pH-modified spray-freeze drying. *Int J Pharm* 2024;**665**:124632.
56. Hassett KJ, Benenato KE, Jacquinet E, Lee A, Woods A, Yuzhakov O, et al. Optimization of lipid nanoparticles for intramuscular administration of mRNA vaccines. *Mol Ther Nucleic Acids* 2019;**15**:1−11.
57. Agency EM. Committee for Medicinal Products for Human Use, EPAR Comirnaty, INN-COVID-19 mRNA vaccine (nucleoside-modified). Available from: https://www.ema.europa.eu/en/documents/assessment-report/comirnaty-epar-public-assessment-report_en.pdf.
58. Di J, Du Z, Wu K, Jin S, Wang X, Li T, et al. Biodistribution and non-linear gene expression of mRNA LNPs affected by delivery route and particle size. *Pharm Res* 2022;**39**:105−14.
59. Chen J, Xu Y, Zhou M, Xu S, Varley AJ, Golubovic A, et al. Combinatorial design of ionizable lipid nanoparticles for muscle-selective mRNA delivery with minimized off-target effects. *Proc Natl Acad Sci U S A* 2023;**120**:e2309472120.
60. Hassett KJ, Rajlic IL, Bahl K, White R, Cowens K, Jacquinet E, et al. mRNA vaccine trafficking and resulting protein expression after intramuscular administration. *Mol Ther Nucleic Acids* 2024;**35**:102083.
61. Lam K, Leung A, Martin A, Wood M, Schreiner P, Palmer L, et al. Unsaturated, trialkyl ionizable lipids are versatile lipid-nanoparticle components for therapeutic and vaccine applications. *Adv Mater* 2023;**35**:e2209624.
62. Sabnis S, Kumarasinghe ES, Salerno T, Mihai C, Ketova T, Senn JJ, et al. A novel amino lipid series for mRNA delivery: improved endosomal escape and sustained pharmacology and safety in non-human primates. *Mol Ther* 2018;**26**:1509−19.
63. Bahl K, Senn JJ, Yuzhakov O, Bulychev A, Brito LA, Hassett KJ, et al. Preclinical and clinical demonstration of immunogenicity by mRNA vaccines against H10N8 and H7N9 influenza viruses. *Mol Ther* 2017;**25**:1316−27.
64. Li S, Hu Y, Li A, Lin J, Hsieh K, Schneiderman Z, et al. Payload distribution and capacity of mRNA lipid nanoparticles. *Nat Commun* 2022;**13**:5561.
65. Kawaguchi M, Noda M, Ono A, Kamiya M, Matsumoto M, Tsurumaru M, et al. Effect of cholesterol content of lipid composition in mRNA-LNPs on the protein expression in the injected site and liver after local administration in mice. *J Pharm Sci* 2023;**112**:1401−10.
66. Carrasco MJ, Alishetty S, Alameh MG, Said H, Wright L, Paige M, et al. Ionization and structural properties of mRNA lipid nanoparticles influence expression in intramuscular and intravascular administration. *Commun Biol* 2021;**4**:956.
67. Long JR, Yu CX, Zhang HL, Cao YM, Sang Y, Lu HT, et al. Novel ionizable lipid nanoparticles for SARS-CoV-2 omicron mRNA delivery. *Adv Healthcare Mater* 2023;**12**:e2202590.
68. Hashiba K, Taguchi M, Sakamoto S, Otsu A, Maeda Y, Suzuki Y, et al. Impact of lipid tail length on the organ selectivity of mRNA-lipid nanoparticles. *Nano Lett* 2024;**24**:12758−67.
69. Rampado R, Naidu GS, Karpov O, Goldsmith M, Sharma P, Ezra A, et al. Lipid nanoparticles with fine-tuned composition show enhanced colon targeting as a platform for mRNA therapeutics. *Adv Sci (Weinh)* 2025;**12**:e2408744.
70. Geng L, Kato N, Kodama Y, Mukai H, Kawakami S. Influence of lipid composition of messenger RNA-loaded lipid nanoparticles on the protein expression *via* intratracheal administration in mice. *Int J Pharm* 2023;**637**:122896.
71. Cui L, Hunter MR, Sonzini S, Pereira S, Romanelli SM, Liu K, et al. Mechanistic studies of an automated lipid nanoparticle reveal critical pharmaceutical properties associated with enhanced mRNA functional delivery *in vitro* and *in vivo*. *Small* 2022;**18**:e2105832.
72. Cheng Q, Wei T, Farbiak L, Johnson LT, Dilliard SA, Siegwart DJ. Selective organ targeting (SORT) nanoparticles for tissue-specific mRNA delivery and CRISPR-cas gene editing. *Nat Nanotechnol* 2020;**15**:313−20.
73. Guéguen C, Ben Chimol T, Briand M, Renaud K, Seiler M, Ziesel M, et al. Evaluating how cationic lipid affects mRNA-LNP physical properties and biodistribution. *Eur J Pharm Biopharm* 2024;**195**:114077.
74. Cheng MHY, Leung J, Zhang Y, Strong C, Basha G, Momeni A, et al. Induction of bleb structures in lipid nanoparticle formulations of mRNA leads to improved transfection potency. *Adv Mater* 2023;**35**:e2303370.
75. Uebbing L, Ziller A, Siewert C, Schroer MA, Blanchet CE, Svergun DI, et al. Investigation of pH-responsiveness inside lipid nanoparticles for parenteral mRNA application using small-angle X-ray scattering. *Langmuir* 2020;**36**:13331−41.
76. Sebastiani F, Yanez Arteta M, Lerche M, Porcar L, Lang C, Bragg RA, et al. Apolipoprotein E binding drives structural and compositional rearrangement of mRNA-containing lipid nanoparticles. *ACS Nano* 2021;**15**:6709−22.
77. Brader ML, Williams SJ, Banks JM, Hui WH, Zhou ZH, Jin L. Encapsulation state of messenger RNA inside lipid nanoparticles. *Biophys J* 2021;**120**:2766−70.
78. Cheng MHY, Zhang Y, Fox K, Leung J, Strong C, Kang E, et al. Liposomal lipid nanoparticles for extrahepatic delivery of mRNA. *Nat Commun* 2025;**16**:4135.
79. Wu KZ, Xu FW, Dai YC, Jin SS, Zheng AJ, Zhang N, et al. Characterization of mRNA-LNP structural features and mechanisms for enhanced mRNA vaccine immunogenicity. *J Control Release* 2024;**376**:1288−99.
80. Melo M, Porter E, Zhang Y, Silva M, Li N, Dobosh B, et al. Immunogenicity of RNA replicons encoding HIV Env immunogens designed for self-assembly into nanoparticles. *Mol Ther* 2019;**27**:2080−90.
81. Pardi N, Tuyishime S, Muramatsu H, Kariko K, Mui BL, Tam YK, et al. Expression kinetics of nucleoside-modified mRNA delivered in lipid nanoparticles to mice by various routes. *J Control Release* 2015;**217**:345−51.
82. Qiu K, Duan X, Mao M, Song Y, Rao Y, Cheng D, et al. mRNA-LNP vaccination-based immunotherapy augments CD8 T cell responses against HPV-positive oropharyngeal cancer. *Npj Vaccines* 2023;**8**:144.
83. ter Haar E, Musacchio A, Harrison SC, Kirchhausen T. Atomic structure of clathrin: a beta propeller terminal domain joins an alpha zigzag linker. *Cell* 1998;**95**:563−73.
84. Kirchhausen T. Imaging endocytic clathrin structures in living cells. *Trends Cell Biol* 2009;**19**:596−605.
85. Hirai Y, Saeki R, Song F, Koide H, Fukata N, Tomita K, et al. Charge-reversible lipid derivative: a novel type of pH-responsive lipid for nanoparticle-mediated siRNA delivery. *Int J Pharm* 2020;**585**:119479.
86. Laatsch A, Panteli M, Sornsakrin M, Hoffzimmer B, Grewal T, Heeren J. Low density lipoprotein receptor-related protein 1 dependent endosomal trapping and recycling of apolipoprotein E. *PLoS One* 2012;**7**:e29385.
87. Tamaru M, Akita H, Kajimoto K, Sato Y, Hatakeyama H, Harashima H. An apolipoprotein E modified liposomal nanoparticle: ligand dependent efficiency as a siRNA delivery carrier for mouse-derived brain endothelial cells. *Int J Pharm* 2014;**465**:77−82.
88. Kim M, Jeong M, Hur S, Cho Y, Park J, Jung H, et al. Engineered ionizable lipid nanoparticles for targeted delivery of RNA

therapeutics into different types of cells in the liver. *Sci Adv* 2021;**7**. eabf4398.
89. Donahue ND, Acar H, Wilhelm S. Concepts of nanoparticle cellular uptake, intracellular trafficking, and kinetics in nanomedicine. *Adv Drug Deliv Rev* 2019;**143**:68−96.
90. Schlich M, Palomba R, Costabile G, Mizrahy S, Pannuzzo M, Peer D, et al. Cytosolic delivery of nucleic acids: the case of ionizable lipid nanoparticles. *Bioeng Transl Med* 2021;**6**:e10213.
91. Paramasivam P, Franke C, Stoter M, Hoijer A, Bartesaghi S, Sabirsh A, et al. Endosomal escape of delivered mRNA from endosomal recycling tubules visualized at the nanoscale. *J Cell Biol* 2022; **221**:e202110137.
92. Sahay G, Querbes W, Alabi C, Eltoukhy A, Sarkar S, Zurenko C, et al. Efficiency of siRNA delivery by lipid nanoparticles is limited by endocytic recycling. *Nat Biotechnol* 2013;**31**:653−8.
93. Patel S, Ashwanikumar N, Robinson E, DuRoss A, Sun C, Murphy-Benenato KE, et al. Boosting intracellular delivery of lipid nanoparticle-encapsulated mRNA. *Nano Lett* 2017;**17**:5711−8.
94. Wittrup A, Ai A, Liu X, Hamar P, Trifonova R, Charisse K, et al. Visualizing lipid-formulated siRNA release from endosomes and target gene knockdown. *Nat Biotechnol* 2015;**33**:870−6.
95. Maugeri M, Nawaz M, Papadimitriou A, Angerfors A, Camponeschi A, Na M, et al. Linkage between endosomal escape of LNP-mRNA and loading into EVs for transport to other cells. *Nat Commun* 2019;**10**:4333.
96. Suzuki Y, Miyazaki T, Muto H, Kubara K, Mukai Y, Watari R, et al. Design and lyophilization of lipid nanoparticles for mRNA vaccine and its robust immune response in mice and nonhuman primates. *Mol Ther Nucl Acids* 2022;**30**:226−40.
97. Fatima M, Park PG, Hong KJ. Clinical advancements in mRNA vaccines against viral infections. *Clin Immunol* 2025;**271**:110424.
98. Shi Y, Shi M, Wang Y, You J. Progress and prospects of mRNA-based drugs in pre-clinical and clinical applications. *Signal Transduct Targeted Ther* 2024;**9**:322.
99. Suzuki Y, Katsurada Y, Hyodo K. Differences and similarities of the intravenously administered lipid nanoparticles in three clinical trials: potential linkage between lipid nanoparticles and extracellular vesicles. *Mol Pharm* 2023;**20**:4883−92.
100. Han X, Alameh MG, Xu Y, Palanki R, El-Mayta R, Dwivedi G, et al. Optimization of the activity and biodegradability of ionizable lipids for mRNA delivery *via* directed chemical evolution. *Nat Biomed Eng* 2024;**8**:1412−24.
101. Sun D, Lu ZR. Structure and function of cationic and ionizable lipids for nucleic acid delivery. *Pharm Res* 2023;**40**:27−46.
102. August A, Attarwala HZ, Himansu S, Kalidindi S, Lu S, Pajon R, et al. A phase 1 trial of lipid-encapsulated mRNA encoding a monoclonal antibody with neutralizing activity against Chikungunya virus. *Nat Med* 2021;**27**:2224−33.
103. Zhang X, Goel V, Robbie GJ. Pharmacokinetics of patisiran, the first approved RNA interference therapy in patients with hereditary transthyretin-mediated amyloidosis. *J Clin Pharmacol* 2020;**60**: 573−85.
104. Administration USFaD. BNT162b2 module 2.6.4. pharmacokinetics written summary. Available from: https://phmpt.org/wp-content/uploads/2022/03/125742_S1_M2_26_pharmkin-written-summary.pdf.
105. Burdette D, Ci L, Shilliday B, Slauter R, Auerbach A, Kenney M, et al. Systemic exposure, metabolism, and elimination of [^{14}C]-labeled amino lipid, lipid 5, after a single administration of mRNA encapsulating lipid nanoparticles to Sprague-Dawley rats. *Drug Metab Dispos* 2023;**51**:804−12.
106. Madi S, Xie F, Farhangi K, Hsu CY, Cheng SH, Aweda T, et al. MRI/PET multimodal imaging of the innate immune response in skeletal muscle and draining lymph node post vaccination in rats. *Front Immunol* 2022;**13**:1081156.
107. Marcos-Contreras OA, Greineder CF, Kiseleva RY, Parhiz H, Walsh LR, Zuluaga-Ramirez V, et al. Selective targeting of nanomedicine to inflamed cerebral vasculature to enhance the blood-brain barrier. *Proc Natl Acad Sci U S A* 2020;**117**:3405−14.
108. Ci L, Hard M, Zhang H, Gandham S, Hua S, Wickwire J, et al. Biodistribution of lipid 5, mRNA, and its translated protein following intravenous administration of mRNA-encapsulated lipid nanoparticles in rats. *Drug Metab Dispos* 2023;**51**:813−23.
109. Christensen J, Litherland K, Faller T, van de Kerkhof E, Natt F, Hunziker J, et al. Biodistribution and metabolism studies of lipid nanoparticle-formulated internally [^{3}H]-labeled siRNA in mice. *Drug Metab Dispos* 2014;**42**:431−40.
110. Vervaeke P, Borgos SE, Sanders NN, Combes F. Regulatory guidelines and preclinical tools to study the biodistribution of RNA therapeutics. *Adv Drug Deliver Rev* 2022;**184**:114236.
111. Solon EG. Autoradiography techniques and quantification of drug distribution. *Cell Tissue Res* 2015;**360**:87−107.
112. Buckley M, Araínga M, Maiorino L, Pires IS, Kim BJ, Michaels KK, et al. Visualizing lipid nanoparticle trafficking for mRNA vaccine delivery in non-human primates. *Mol Ther* 2025;**33**:1105−17.
113. Lindsay KE, Bhosle SM, Zurla C, Beyersdorf J, Rogers KA, Vanover D, et al. Visualization of early events in mRNA vaccine delivery in non-human primates *via* PET-CT and near-infrared imaging. *Nat Biomed Eng* 2019;**3**:371−80.
114. Christensen J, Litherland K, Faller T, van de Kerkhof E, Natt F, Hunziker J, et al. Metabolism studies of unformulated internally [^{3}H]-labeled short interfering RNAs in mices. *Drug Metab Dispos* 2013;**41**:1211−9.
115. Sandelius Å, Naseer H, Lindqvist J, Wilson A, Henderson N. Biodistribution of lipid nanoparticle, *eGFP* mRNA and translated protein following subcutaneous administration in mouse. *Bioanalysis* 2024; **16**:721−33.
116. Eberlin LS, Ferreira CR, Dill AL, Ifa DR, Cooks RG. Desorption electrospray ionization mass spectrometry for lipid characterization and biological tissue imaging. *Bba-Mol Cell Biol L* 2011;**1811**: 946−60.
117. Cologna SM. Mass spectrometry imaging of cholesterol. *Adv Exp Med Biol* 2019;**1115**:155−66.
118. Züllig T, Köfeler HC. High resolution mass spectrometry in lipidomics. *Mass Spectrom Rev* 2021;**40**:162−76.
119. Fekete S, Doneanu C, Addepalli B, Gaye M, Nguyen J, Alden B, et al. Challenges and emerging trends in liquid chromatography-based analyses of mRNA pharmaceuticals. *J Pharm Biomed Anal* 2023;**224**:115174.
120. Lowenthal MS, Antonishek AS, Phinney KW. Quantification of mRNA in lipid nanoparticles using mass spectrometry. *Anal Chem* 2024;**96**:1214−22.
121. Sutton WJH, Branham PJ, Williamson YM, Cooper HC, Najjar FN, Pierce-Ruiz CL, et al. Quantification of SARS-CoV-2 spike protein expression from mRNA vaccines using isotope dilution mass spectrometry. *Vaccine* 2023;**41**:3872−84.
122. Qiu M, Tang Y, Chen JJ, Muriph R, Ye ZF, Huang CF, et al. Lung-selective mRNA delivery of synthetic lipid nanoparticles for the treatment of pulmonary lymphangioleiomyomatosis. *Proc Natl Acad Sci U S A* 2022;**119**:e2116271119.
123. Luo PK, Ho HM, Chiang MC, Chu LA, Chuang YH, Lyu PC, et al. pH-responsive β-glucans-complexed mRNA in LNPs as an oral vaccine for enhancing cancer immunotherapy. *Adv Mater* 2024;**36**: e2404830.
124. Xue LL, Gong NQ, Shepherd SJ, Xiong XH, Liao XY, Han XX, et al. Rational design of bisphosphonate lipid-like materials for mRNA delivery to the bone microenvironment. *J Am Chem Soc* 2022;**144**: 9926−37.
125. Mérian J, Boisgard R, Bayle PA, Bardet M, Tavitian B, Texier I. Comparative biodistribution in mice of cyanine dyes loaded in lipid nanoparticles. *Eur J Pharm Biopharm* 2015;**93**:1−10.
126. Baladi T, Nilsson JR, Gallud A, Celauro E, Gasse C, Levi-Acobas F, et al. Stealth fluorescence labeling for live microscopy imaging of mRNA delivery. *J Am Chem Soc* 2021;**143**:5413−24.

127. Wang B, Chen Z, Ren D, You Z. A novel dual energy transfer probe for intracellular mRNA detection with high robustness and specificity. *Sens Actuators B Chem* 2019;**279**:342−50.
128. Chen X, Zhang D, Su N, Bao B, Xie X, Zuo F, et al. Visualizing RNA dynamics in live cells with bright and stable fluorescent RNAs. *Nat Biotechnol* 2019;**37**:1287−93.
129. Mamot A, Sikorski PJ, Warminski M, Kowalska J, Jemielity J. Azido-functionalized 5′ cap analogues for the preparation of translationally active mRNAs suitable for fluorescent labeling in living cells. *Angew Chem Int Ed Engl* 2017;**56**:15628−32.
130. Anhäuser L, Hüwel S, Zobel T, Rentmeister A. Multiple covalent fluorescence labeling of eukaryotic mRNA at the poly(A) tail enhances translation and can be performed in living cells. *Nucleic Acids Res* 2019;**47**:e42.
131. Saito K, Nagai T. Recent progress in luminescent proteins development. *Curr Opin Chem Biol* 2015;**27**:46−51.
132. Parhiz H, Shuvaev VV, Li Q, Papp TE, Akyianu AA, Shi R, et al. Physiologically based modeling of LNP-mediated delivery of mRNA in the vascular system. *Mol Ther Nucleic Acids* 2024;**35**:102175.
133. Ma R, Li Y, Wei Y, Zhou J, Ma J, Zhang M, et al. The dynamic process of mRNA delivery by lipid nanoparticles *in vivo*. *Nano Today* 2024;**57**:102325.
134. Ignowski JM, Schaffer DV. Kinetic analysis and modeling of firefly luciferase as a quantitative reporter gene in live mammalian cells. *Biotechnol Bioeng* 2004;**86**:827−34.
135. Li W, Kitsios GD, Bain W, Wang C, Li T, Fanning KV, et al. Stability of SARS-CoV-2-encoded proteins and their antibody levels correlate with interleukin 6 in COVID-19 patients. *mSystems* 2022;**7**: e0005822.
136. Greig JA, Jennis M, Dandekar A, Chorazeczewski JK, Param N, So MR, et al. Lipid nanoparticle mRNA therapy improves survival and reduces serum branched-chain amino acids in mouse models of maple syrup urine disease. *Hum Gene Ther* 2024;**35**:726−33.
137. An D, Schneller JL, Frassetto A, Liang S, Zhu XL, Park JS, et al. Systemic messenger RNA therapy as a treatment for methylmalonic acidemia. *Cell Rep* 2017;**21**:3548−58.
138. Young AP, Jackson DJ, Wyeth RC. A technical review and guide to RNA fluorescence *in situ* hybridization. *PeerJ* 2020;**8**:e8806.
139. Tutucci E, Livingston NM, Singer RH, Wu B. Imaging mRNA *in vivo*, from birth to death. *Annu Rev Biophys* 2018;**47**:85−106.
140. Arrigucci R, Bushkin Y, Radford F, Lakehal K, Vir P, Pine R, et al. FISH-Flow, a protocol for the concurrent detection of mRNA and protein in single cells using fluorescence hybridization and flow cytometry. *Nat Protoc* 2017;**12**:1245−60.
141. Sedic M, Senn JJ, Lynn A, Laska M, Smith M, Platz SJ, et al. Safety evaluation of lipid nanoparticle-formulated modified mRNA in the Sprague-Dawley rat and cynomolgus monkey. *Vet Pathol* 2018;**55**: 341−54.
142. Agency EM. Committee for Medicinal Products for Human Use, EPAR COVID-19 vaccine Moderna, INN-COVID-19 mRNA vaccine (nucleoside modified). Available from: https://www.ema.europa.eu/en/documents/assessment-report/spikevax-previously-covid-19-vaccine-moderna-epar-public-assessment-report_en.pdf.
143. Henderson N, Wilson A. Measurement of mRNA therapeutics: method development and validation challenges. *Bioanalysis* 2019;**11**: 2003−10.
144. Lourenc Correia Moreira B, Aparecida Pereira L, Lappas Gimenez AP, Minor Fernandes Inagaki J, Raboni SM. Development and validation of a real-time RT-PCR assay for the quantification of rabies virus as quality control of inactivated rabies vaccines. *J Virol Methods* 2019;**270**:46−51.
145. Ortiz J, Brunner L, Ci L, Baek R, Jani D, Marshall JC, et al. Comparison of RT-qPCR with branched DNA to quantify a lipid nanoparticle-encapsulated mRNA therapeutic in serum and liver tissue samples from nonclinical PK studies. *AAPS J* 2025;**27**:27.
146. Liu D, Wang X, Xu L, Al-Delfi ZNS, Mekonnen ZA, Gao S, et al. Screening lipid nanoparticles using DNA barcoding and qPCR. *Colloids Surf B Biointerfaces* 2025;**251**:114598.
147. Zhang HQ, Gao X, Sun Q, Dong XX, Zhu ZW, Yang CX. Incorporation of poly(γ-glutamic acid) in lipid nanoparticles for enhanced mRNA delivery efficiency *in vitro* and *in vivo*. *Acta Biomater* 2024; **177**:361−76.
148. Rahbar Z, Nazarian S, Dorostkar R, Sotoodehnejadnematalahi F, Amani J. Recombinant expression of SARS-CoV-2 receptor binding domain (RBD) in and its immunogenicity in mice. *Iran J Basic Med Sci* 2022;**25**:1110−6.
149. Pratesi F, Caruso T, Testa D, Tarpanelli T, Gentili A, Gioè D, et al. BNT162b2 mRNA SARS-CoV-2 vaccine elicits high avidity and neutralizing antibodies in healthcare workers. *Vaccines* 2021;**9**:672.
150. Zhang NN, Li XF, Deng YQ, Zhao H, Huang YJ, Yang G, et al. A thermostable mRNA vaccine against COVID-19. *Cell* 2020;**182**: 1271−83.
151. Yeo KT, Chia WN, Tan CW, Ong C, Yeo JG, Zhang J, et al. Neutralizing activity and SARS-CoV-2 vaccine mRNA persistence in serum and breastmilk after BNT162b2 vaccination in lactating women. *Front Immunol* 2021;**12**:783975.
152. Munro APS, Feng S, Janani L, Cornelius V, Aley PK, Babbage G, et al. Safety, immunogenicity, and reactogenicity of BNT162b2 and mRNA-1273 COVID-19 vaccines given as fourth-dose boosters following two doses of ChAdOx1 nCoV-19 or BNT162b2 and a third dose of BNT162b2 (COV-BOOST): a multicentre, blinded, phase 2, randomised trial. *Lancet Infect Dis* 2022;**22**:1131−41.
153. Sohi AN, Kiani J, Arefian E, Khosrojerdi A, Fekrirad Z, Ghaemi S, et al. Development of an mRNA-LNP vaccine against SARS-CoV-2: evaluation of immune response in mouse and rhesus macaque. *Vaccines* 2021;**9**:1007.
154. Lim XR, Tan JWL, Chan GYL, Hou J, Xie L, Goh VHL, et al. Evaluation of patients with vaccine allergies prior to mRNA-based COVID-19 vaccination. *Vaccines (Basel)* 2022;**10**:1025.
155. Carreño JM, Singh G, Tcheou J, Srivastava K, Gleason C, Muramatsu H, et al. mRNA-1273 but not BNT162b2 induces antibodies against polyethylene glycol (PEG) contained in mRNA-based vaccine formulations. *Vaccine* 2022;**40**:6114−24.
156. Huayamares SG, Lokugamage MP, Rab R, Sanchez AJD, Kim H, Radmand A, et al. High-throughput screens identify a lipid nanoparticle that preferentially delivers mRNA to human tumors *in vivo*. *J Control Release* 2023;**357**:394−403.
157. Sanchez AJD, Zhao K, Huayamares SG, Hatit MZC, Lokugamage MP, Loughrey D, et al. Substituting racemic ionizable lipids with stereopure ionizable lipids can increase mRNA delivery. *J Control Release* 2023;**353**:270−7.
158. Rhym LH, Manan RS, Koller A, Stephanie G, Anderson DG. Peptide-encoding mRNA barcodes for the high-throughput *in vivo* screening of libraries of lipid nanoparticles for mRNA delivery. *Nat Biomed Eng* 2023;**7**:901−10.
159. Wang KV, Young TL, Chen JG, Tsai SN, Xu Y, Varley AJ, et al. A reverse transcription nucleic-acid-based barcoding system for measurement of lipid nanoparticle mRNA delivery. *Acs Bio Med Chem Au* 2025;**5**:35−41.
160. Dane EL, Pote AR, Hemmerling M, Czechtizky W, Zhou LP, Bak A. New ionizable lipids for non-viral mRNA delivery with secondary amine cyclic ether head groups. *RSC Med Chem* 2025;**16**:3273−80.
161. Wang M, Sun S, Alberti KA, Xu QB. A combinatorial library of unsaturated lipidoids for efficient intracellular gene delivery. *ACS Synth Biol* 2012;**1**:403−7.
162. Lee SM, Cheng Q, Yu XL, Liu S, Johnson LT, Siegwart DJ. A systematic study of unsaturation in lipid nanoparticles leads to improved mRNA transfection *in vivo*. *Angew Chem Int Ed* 2021;**60**: 5848−53.
163. Liu C, Jiang YH, Xue WL, Liu JY, Wang ZH, Li XS. Multiple tail ionizable lipids improve *in vivo* mRNA delivery efficiency with biosafety. *Int J Pharmaceut* 2024;**667**:124868.
164. Mrksich K, Padilla MS, Joseph RA, Han EL, Kim D, Palanki R, et al. Influence of ionizable lipid tail length on lipid nanoparticle delivery of mRNA of varying length. *J Biomed Mater Res* 2024;**112**: 1494−505.

165. Liu JW, Sun WJ, Xiao B, Xu HR, Fan JQ, Shi XY, et al. Ionizable lipids with branched linkers enhance the delivery of mRNA vaccines. *Acs Appl Mater Inter* 2025;**17**:13552−64.
166. Chen ZM, Tian Y, Yang JY, Wu FP, Liu SY, Cao WW, et al. Modular design of biodegradable ionizable lipids for improved mRNA delivery and precise cancer metastasis delineation *in vivo*. *J Am Chem Soc* 2023;**145**:24302−14.
167. Lv K, Yu Z, Wang J, Li N, Wang A, Xue T, et al. Discovery of ketal-ester ionizable lipid nanoparticle with reduced hepatotoxicity, enhanced spleen tropism for mRNA vaccine delivery. *Adv Sci (Weinh)* 2024;**11**:e2404684.
168. Huo HA, Cheng XD, Xu JX, Lin JQ, Chen N, Lu XG. A fluorinated ionizable lipid improves the mRNA delivery efficiency of lipid nanoparticles. *J Mater Chem B* 2023;**11**:4171−80.
169. Wang CL, Zhou YM, Gao YX, Pan XP, Jia WL, Wu TJ, et al. Lipid nanoparticles consisting of sterol-conjugated ionizable lipids enable prolonged and safe mRNA delivery. *Acs Appl Mater Inter* 2025;**17**:37763−73.
170. Jung O, Jung HY, Thuy LT, Choi M, Kim S, Jeon HG, et al. Modulating lipid nanoparticles with histidinamide-conjugated cholesterol for improved intracellular delivery of mRNA. *Adv Healthcare Mater* 2024;**13**:e2303857.
171. Patel S, Ashwanikumar N, Robinson E, Xia Y, Mihai C, Griffith 3rd JP, et al. Author correction: Naturally-occurring cholesterol analogues in lipid nanoparticles induce polymorphic shape and enhance intracellular delivery of mRNA. *Nat Commun* 2020;**11**:3435.
172. Bogaert B, Debisschop A, Ehouarne T, Van Eeckhoutte HP, De Volder J, Jacobs A, et al. Selective replacement of cholesterol with cationic amphiphilic drugs enables the design of lipid nanoparticles with improved RNA delivery. *Nano Lett* 2024;**24**:2961−71.
173. Sedlmayr VL, Schobesberger S, Spitz S, Ertl P, Wurm DJ, Quehenberger J, et al. Archaeal ether lipids improve internalization and transfection with mRNA lipid nanoparticles. *Eur J Pharm Biopharm* 2024;**197**:114213.
174. Soh WWM, Finol E, Chan SJW, Zhu JY, Liau S, Bier A, et al. Tailoring lipid nanoparticle with *ex situ* incorporated conjugated oligoelectrolyte for enhanced mRNA delivery efficiency. *Adv Healthcare Mater* 2025;**14**:e2405048.
175. Zeng Y, Shen MJ, Pattipeiluhu R, Zhou XQ, Zhang Y, Bakkum T, et al. Efficient mRNA delivery using lipid nanoparticles modified with fusogenic coiled-coil peptides. *Nanoscale* 2023;**15**:15206−18.
176. Wang C, Zhao C, Wang W, Liu X, Deng H. Biomimetic noncationic lipid nanoparticles for mRNA delivery. *Proc Natl Acad Sci U S A* 2023;**120**:e2311276120.
177. Han X, Alameh MG, Butowska K, Knox JJ, Lundgreen K, Ghattas M, et al. Adjuvant lipidoid-substituted lipid nanoparticles augment the immunogenicity of SARS-CoV-2 mRNA vaccines. *Nat Nanotechnol* 2023;**18**:1105−14.
178. Misra B, Hughes KA, Pentz WH, Surface M, Geldenhuys WJ, Bobbala S. TLR7-adjuvanted ionizable lipid nanoparticles for mRNA vaccine delivery. *AAPS J* 2025;**27**:80.
179. Yong SB, Ha M, Cho SC. Microbiome metabolite-incorporated lipid nanoparticles augment CD8 T cell memory potential and immunity for mRNA cancer vaccines. *ACS Biomater Sci Eng* 2025;**11**:4254−65.
180. Bachem A, Makhlouf C, Binger KJ, de Souza DP, Tull D, Hochheiser K, et al. Microbiota-derived short-chain fatty acids promote the memory potential of antigen-activated CD8 T cells. *Immunity* 2019;**51**:285−97.e5.
181. Denk D, Petrocelli V, Conche C, Drachsler M, Ziegler PK, Braun A, et al. Expansion of T memory stem cells with superior anti-tumor immunity by urolithin a-induced mitophagy. *Immunity* 2022;**55**:2059−73.e8.
182. Li L, Luo M, Zhou L, Wang Y, Jiao Y, Wang C, et al. Glucocorticoid pre-administration improves LNP-mRNA mediated protein replacement and genome editing therapies. *Int J Pharm* 2025;**672**:125282.
183. Park H, Kang I, Lee S, Park M, Kim S, Lim SY, et al. Local delivery of *IL-12* mRNA and indoximod prodrug potentiates antitumor immunity by increasing T cell effector function. *J Control Release* 2025;**385**:113970.
184. Gong N, Zhong W, Alameh MG, Han X, Xue L, El-Mayta R, et al. Tumour-derived small extracellular vesicles act as a barrier to therapeutic nanoparticle delivery. *Nat Mater* 2024;**23**:1736−47.
185. Xue LL, Xiong XH, Zhao G, Molina-Arocho W, Palanki R, Xiao ZB, et al. Multiarm-assisted design of dendron-like degradable ionizable lipids facilitates systemic mRNA delivery to the spleen. *J Am Chem Soc* 2025;**147**:1542−52.
186. Wu SQ, Shi L, Su KX, Lin LX, Yan XX, Zhang YR, et al. Carbonate-bearing ionizable lipids for mRNA delivery to splenic NK cells. *J Am Chem Soc* 2025;**147**:28665−73.
187. Kim M, Jeong M, Lee G, Lee Y, Park J, Jung H, et al. Novel piperazine-based ionizable lipid nanoparticles allow the repeated dose of mRNA to fibrotic lungs with improved potency and safety. *Bioeng Transl Med* 2023;**8**:e10556.
188. Somu Naidu G, Rampado R, Sharma P, Ezra A, Kundoor GR, Breier D, et al. Ionizable lipids with optimized linkers enable lung-specific, lipid nanoparticle-mediated mRNA delivery for treatment of metastatic lung tumors. *ACS Nano* 2025;**19**:6571−87.
189. Dilliard SA, Cheng Q, Siegwart DJ. On the mechanism of tissue-specific mRNA delivery by selective organ targeting nanoparticles. *Proc Natl Acad Sci U S A* 2021;**118**:e2109256118.
190. Liu C, Jiang YH, Xue WL, Liu JY, Wang ZH, Luo JH, et al. Ionizable cholesterol analogs as the fifth component of lipid nanoparticles for selective targeting delivery of mRNA. *ACS Appl Mater Interfaces* 2025;**17**:4416−25.
191. Sahoo D, Atochina-Vasserman EN, Maurya DS, Arshad M, Chenna SS, Ona N, et al. The constitutional isomerism of one-component ionizable amphiphilic janus dendrimers orchestrates the total and targeted activities of mRNA delivery. *J Am Chem Soc* 2024;**146**:3627−34.
192. Zhang DP, Atochina-Vasserman EN, Maurya DS, Liu M, Xiao Q, Lu JC, et al. Targeted delivery of mRNA with one-component ionizable amphiphilic janus dendrimers. *J Am Chem Soc* 2021;**143**:17975−82.
193. Lin L, Su K, Zhang X, Shi L, Yan X, Fu Q, et al. A versatile strategy to transform cationic polymers for efficient and organ-selective mRNA delivery. *Angew Chem Int Ed Engl* 2025;**64**:e202500306.
194. Espinar AL, Mulder LM, Elkhashab M, Khan Z, Czarnocki-Cieciura M, Aburto MR, et al. Tailoring alkyl side chains of ionizable amino-polyesters for enhanced *in vivo* mRNA delivery. *ACS Appl Bio Mater* 2025;**8**:3958−71.
195. Lokugamage MP, Vanover D, Beyersdorf J, Hatit MZC, Rotolo L, Echeverri ES, et al. Optimization of lipid nanoparticles for the delivery of nebulized therapeutic mRNA to the lungs. *Nat Biomed Eng* 2021;**5**:1059−68.
196. Li B, Manan RS, Liang SQ, Gordon A, Jiang A, Varley A, et al. Combinatorial design of nanoparticles for pulmonary mRNA delivery and genome editing. *Nat Biotechnol* 2023;**41**:1410−5.
197. Bai X, Chen Q, Li F, Teng Y, Tang M, Huang J, et al. Optimized inhaled LNP formulation for enhanced treatment of idiopathic pulmonary fibrosis *via* mRNA-mediated antibody therapy. *Nat Commun* 2024;**15**:6844.
198. Massaro M, Wu S, Baudo G, Liu H, Collum S, Lee H, et al. Lipid nanoparticle-mediated mRNA delivery in lung fibrosis. *Eur J Pharmaceut Sci* 2023;**183**:106370.
199. Isaac I, Patel L, Tran N, Singam A, Yun D, Guha P, et al. Reengineering endogenous targeting lipid nanoparticles (endo) for systemic delivery of mRNA to pancreas. *Adv Mater* 2025;**37**:e2507657.
200. Farrell KB, Karpeisky A, Thamm DH, Zinnen S. Bisphosphonate conjugation for bone specific drug targeting. *Bone Reports* 2018;**9**:47−60.
201. Yoon IC, Xue L, Chen Q, Liu J, Xu J, Siddiqui Z, et al. Piperazine-derived bisphosphonate-based ionizable lipid nanoparticles enhance

mRNA delivery to the bone microenvironment. *Angew Chem Int Ed Engl* 2025;**64**:e202415389.
202. Lian XZ, Chatterjee S, Sun YH, Dilliard SA, Moore S, Xiao YF, et al. Bone-marrow-homing lipid nanoparticles for genome editing in diseased and malignant haematopoietic stem cells. *Nat Nanotechnol* 2024;**19**:1409−17.
203. Zhao XW, Chen JJ, Qiu M, Li YM, Glass Z, Xu QB. Imidazole-based synthetic lipidoids for *in vivo* mRNA delivery into primary T lymphocytes. *Angew Chem Int Ed* 2020;**59**:20083−9.
204. Fenton OS, Kauffman KJ, Kaczmarek JC, McClellan RL, Jhunjhunwala S, Tibbitt MW, et al. Synthesis and biological evaluation of ionizable lipid materials for the *in vivo* delivery of messenger RNA to B lymphocytes. *Adv Mater* 2017;**29**:1606944.
205. Suzuki Y, Yakuwa M, Sato M, Samaridou E, Beck-Broichsitter M, Maeki M, et al. Splenic B cell-targeting lipid nanoparticles for safe and effective mRNA vaccine delivery. *J Control Release* 2025;**382**: 113687.
206. Ma T, Chen X, Wang M. Intracellular delivery of mRNA for cell-selective CRISPR/cas9 genome editing using lipid nanoparticles. *Chembiochem* 2023;**24**:e202200801.
207. Tang Q, Liu J, Jiang Y, Zhang MN, Mao LQ, Wang M. Cell-selective messenger RNA delivery and CRISPR/cas9 genome editing by modulating the interface of phenylboronic acid-derived lipid nanoparticles and cellular surface sialic acid. *Acs Appl Mater Inter* 2019; **11**:46585−90.
208. Zeng JY, Lingesh S, Krishnan NB, Loong BSY, Liu M, Chen Q, et al. Cholesterol-derived mannosylated polypeptide-formed lipid nanoparticles for efficient *in vivo* mRNA delivery. *Small Methods* 2025;**9**: e2401712.
209. Rurik JG, Tombácz I, Yadegari A, Méndez Fernández PO, Shewale SV, Li L, et al. CAR T cells produced *in vivo* to treat cardiac injury. *Science* 2022;**375**:91−6.
210. Rosenblum D, Gutkin A, Kedmi R, Ramishetti S, Veiga N, Jacobi AM, et al. CRISPR-cas9 genome editing using targeted lipid nanoparticles for cancer therapy. *Sci Adv* 2020;**6**. eabc9450.
211. Shi D, Toyonaga S, Anderson DG. *In vivo* RNA delivery to hematopoietic stem and progenitor cells *via* targeted lipid nanoparticles. *Nano Lett* 2023;**23**:2938−44.
212. Papp TE, Zeng J, Shahnawaz H, Akyianu A, Breda L, Yadegari A, et al. CD47 peptide-cloaked lipid nanoparticles promote cell-specific mRNA delivery. *Mol Ther* 2025;**33**:3195−208.
213. Münter R, Christensen E, Andresen TL, Larsen JB. Studying how administration route and dose regulates antibody generation against LNPs for mRNA delivery with single-particle resolution. *Mol Ther, Methods Clin Dev* 2023;**29**:450−9.
214. Ishida T, Harada M, Wang XY, Ichihara M, Irimura K, Kiwada H. Accelerated blood clearance of PEGylated liposomes following preceding liposome injection: effects of lipid dose and PEG surface-density and chain length of the first-dose liposomes. *J Control Release* 2005;**105**:305−17.
215. Wang H, Wang Y, Yuan C, Xu X, Zhou W, Huang Y, et al. Polyethylene glycol (PEG)-associated immune responses triggered by clinically relevant lipid nanoparticles in rats. *Npj Vaccines* 2023;**8**: 169.
216. Kozma GT, Mészáros T, Berényi P, Facskó R, Patkó Z, Oláh CZ, et al. Role of anti-polyethylene glycol (PEG) antibodies in the allergic reactions to PEG-containing Covid-19 vaccines: evidence for immunogenicity of PEG. *Vaccine* 2023;**41**:4561−70.
217. Suzuki T, Suzuki Y, Hihara T, Kubara K, Kondo K, Hyodo K, et al. PEG shedding-rate-dependent blood clearance of PEGylated lipid nanoparticles in mice: faster PEG shedding attenuates anti-PEG IgM production. *Int J Pharm* 2020;**588**:119792.
218. Mima Y, Hashimoto Y, Shimizu T, Kiwada H, Ishida T. Anti-PEG IgM is a major contributor to the accelerated blood clearance of polyethylene glycol-conjugated protein. *Mol Pharm* 2015;**12**: 2429−35.
219. Sui DZ, Wang YJ, Sun WL, Wei L, Li CZ, Gui YX, et al. Cleavable-branched polymer-modified liposomes reduce accelerated blood clearance and enhance photothermal therapy. *Acs Appl Mater Inter* 2023;**15**:32110−20.
220. Zhang Z, Chu YX, Li C, Tang WJ, Qian J, Wei XL, et al. Anti-PEG scFv corona ameliorates accelerated blood clearance phenomenon of PEGylated nanomedicines. *J Control Release* 2021;**330**:493−501.
221. Sanchez A, Loughrey D, Echeverri ES, Huayamares SG, Radmand A, Paunovska K, et al. Substituting poly(ethylene glycol) lipids with poly(2-ethyl-2-oxazoline) lipids improves lipid nanoparticle repeat dosing. *Adv Healthcare Mater* 2024;**13**:e2304033.
222. Holick CT, Klein T, Mehnert C, Adermann F, Anufriev I, Streiber M, et al. Poly(2-ethyl-2-oxazoline) (pox) as poly(ethylene glycol) (PEG)-lipid substitute for lipid nanoparticle formulations. *Small* 2025;**21**:e2411354.
223. Yao X, Qi C, Sun C, Huo F, Jiang X. Poly(ethylene glycol) alternatives in biomedical applications. *Nano Today* 2023;**48**:101738.
224. Song JX, Su DH, Wu HB, Guo JRY. Implications of anaphylaxis following mRNA-LNP vaccines: it is urgent to eliminate PEG and find alternatives. *Pharmaceutics* 2025;**17**:798.
225. Kang DD, Hou XC, Wang LM, Xue YE, Li HY, Zhong YC, et al. Engineering LNPs with polysarcosine lipids for mRNA delivery. *Bioact Mater* 2024;**37**:86−93.
226. Nogueira SS, Schlegel A, Maxeiner K, Weber B, Barz M, Schroer MA, et al. Polysarcosine-functionalized lipid nanoparticles for therapeutic mRNA delivery. *ACS Appl Nano Mater* 2020;**3**: 10634−45.
227. Son K, Ueda M, Taguchi K, Maruyama T, Takeoka S, Ito Y. Evasion of the accelerated blood clearance phenomenon by polysarcosine coating of liposomes. *J Control Release* 2020;**322**:209−16.
228. Luozhong SJ, Liu PC, Li RX, Yuan ZF, Debley E, Chen Y, et al. Poly (carboxybetaine) lipids enhance mRNA therapeutics efficacy and reduce their immunogenicity. *Nat Mater* 2025. Available from: https://doi.org/10.1038/s41563-025-02240-8.
229. Xiao YF, Lian XZ, Sun YH, Sung YC, Vaidya A, Chen ZX, et al. High-density brush-shaped polymer lipids reduce anti-PEG antibody binding for repeated administration of mRNA therapeutics. *Nat Mater* 2025. Available from: https://doi.org/10.1038/s41563-024-02116-3.
230. Chen S, Zaifman J, Kulkarni JA, Zhigaltsev IV, Tam YK, Ciufolini MA, et al. Dexamethasone prodrugs as potent suppressors of the immunostimulatory effects of lipid nanoparticle formulations of nucleic acids. *J Control Release* 2018;**286**:46−54.
231. Vlatkovic I. Non-immunotherapy application of LNP-mRNA: maximizing efficacy and safety. *Biomedicines* 2021;**9**:530.
232. Verbeke R, Hogan MJ, Loré K, Pardi N. Innate immune mechanisms of mRNA vaccines. *Immunity* 2022;**55**:1993−2005.
233. Tahtinen S, Tong AJ, Himmels P, Oh J, Paler-Martinez A, Kim L, et al. IL-1 and IL-1ra are key regulators of the inflammatory response to RNA vaccines. *Nat Immunol* 2022;**23**:532−42.
234. Huang P, Jiang L, Pan H, Ding L, Zhou B, Zhao M, et al. An integrated polymeric mRNA vaccine without inflammation side effects for cellular immunity mediated cancer therapy. *Adv Mater* 2023;**35**: e2207471.
235. Chaudhary N, Kasiewicz LN, Newby AN, Arral ML, Yerneni SS, Melamed JR, et al. Amine headgroups in ionizable lipids drive immune responses to lipid nanoparticles by binding to the receptors TLR4 and CD1d. *Nat Biomed Eng* 2024;**8**:1483−98.
236. Matayoshi K, Takahashi S, Ryu S, Koide H, Yonezawa S, Ozaki N, et al. Development of a messenger RNA vaccine using pH-responsive dipeptide-conjugated lipids exhibiting reduced inflammatory properties. *Int J Pharm* 2025;**674**:125485.
237. Bae SH, Yoo S, Lee J, Park HJ, Kwon SP, Jin HR, et al. A lipid nanoparticle platform incorporating trehalose glycolipid for exceptional mRNA vaccine safety. *Bioact Mater* 2024;**38**:486−98.
238. Liu JW, Xiao B, Yang YL, Jiang YF, Wang R, Wei Q, et al. Low-dose mildronate-derived lipidoids for efficient mRNA vaccine delivery with minimal inflammation side effects. *ACS Nano* 2024;**18**: 23289−300.
239. Popowski KD, López de Juan Abad B, George A, Silkstone D, Belcher E, Chung J, et al. Inhalable exosomes outperform liposomes

as mRNA and protein drug carriers to the lung. *Extracell vesicle* 2022;**1**:100002.
240. Wang JH, Forterre AV, Zhao JJ, Frimannsson DO, Delcayre A, Antes TJ, et al. Anti-HER2 scFv-directed extracellular vesicle-mediated mRNA-based gene delivery inhibits growth of HER2-positive human breast tumor xenografts by prodrug activation. *Mol Cancer Therapeut* 2018;**17**:1133−42.
241. Altanerova U, Jakubechova J, Benejova K, Petra P, Pesta M, Pitule P, et al. Prodrug suicide gene therapy for cancer targeted intracellular by mesenchymal stem cell exosomes. *Int J Cancer* 2019;**144**: 897−908.
242. Kojima R, Bojar D, Rizzi G, Hamri GC, El-Baba MD, Saxena P, et al. Designer exosomes produced by implanted cells intracerebrally deliver therapeutic cargo for Parkinson's disease treatment. *Nat Commun* 2018;**9**:1305.
243. You Y, Tian Y, Yang Z, Shi J, Kwak KJ, Tong Y, et al. Intradermally delivered mRNA-encapsulating extracellular vesicles for collagen-replacement therapy. *Nat Biomed Eng* 2023;**7**:887−900.
244. Dong S, Liu X, Bi Y, Wang Y, Antony A, Lee D, et al. Adaptive design of mRNA-loaded extracellular vesicles for targeted immunotherapy of cancer. *Nat Commun* 2023;**14**:6610.
245. Wan Y, Li L, Chen R, Han J, Lei Q, Chen Z, et al. Engineered extracellular vesicles efficiently deliver CRISPR-cas9 ribonucleoprotein (RNP) to inhibit herpes simplex virus1 infection *in vitro* and *in vivo*. *Acta Pharm Sin B* 2024;**14**:1362−79.
246. Adlsadabad SY, Hanrahan JW, Kakkar A. mRNA delivery: challenges and advances through polymeric soft nanoparticles. *Int J Mol Sci* 2024;**25**:1739.
247. Li XD, Le Y, Zhang ZG, Nian XX, Liu B, Yang XM. Viral vector-based gene therapy. *Int J Mol Sci* 2023;**24**:7736.
248. Travieso T, Li J, Mahesh S, Mello J, Blasi M. The use of viral vectors in vaccine development. *Npj Vaccines* 2022;**7**:75.
249. Verdera HC, Kuranda K, Mingozzi F. AAV vector immunogenicity in humans: a long journey to successful gene transfer. *Mol Ther* 2020; **28**:723−46.
250. Brown DW, Wee P, Bhandari P, Bukhari A, Grin L, Vega H, et al. Safe and effective *in vivo* delivery of DNA and RNA using proteolipid vehicles. *Cell* 2024;**187**:5357−75.e24.
251. Maeki M, Uno S, Sugiura K, Sato Y, Fujioka Y, Ishida A, et al. Development of polymer-lipid hybrid nanoparticles for large-sized plasmid DNA transfection. *ACS Appl Mater Interfaces* 2024;**16**: 2110−9.
252. Das R, Halabi EA, Fredrich IR, Oh J, Peterson HM, Ge X, et al. Hybrid LNP prime dendritic cells for nucleotide delivery. *Adv Sci (Weinh)* 2023;**10**:e2303576.
253. Rodríguez DA, Vader P. Extracellular vesicle-based hybrid systems for advanced drug delivery. *Pharmaceutics* 2022;**14**:267.
254. Gu W, Luozhong S, Cai S, Londhe K, Elkasri N, Hawkins R, et al. Extracellular vesicles incorporating retrovirus-like capsids for the enhanced packaging and systemic delivery of mRNA into neurons. *Nat Biomed Eng* 2024;**8**:415−26.
255. Yan Y, Du C, Duan X, Yao X, Wan J, Jiang Z, et al. Inhibiting collagen I production and tumor cell colonization in the lung *via* miR-29a-3p loading of exosome-/liposome-based nanovesicles. *Acta Pharm Sin B* 2022;**12**:939−51.
256. Sivadasan D, Sultan MH, Madkhali O, Almoshari Y, Thangavel N. Polymeric lipid hybrid nanoparticles (PLNs) as emerging drug delivery platform—a comprehensive review of their properties, preparation methods, and therapeutic applications. *Pharmaceutics* 2021; **13**:1291.
257. Gajbhiye KR, Salve R, Narwade M, Sheikh A, Kesharwani P, Gajbhiye V. Lipid polymer hybrid nanoparticles: a custom-tailored next-generation approach for cancer therapeutics. *Mol Cancer* 2023;**22**:160.
258. Shen S, Li T, Fan J, Shao Q, Dong H, Xu X, et al. Lipid-polymer hybrid nanoparticle with cell-distinct drug release for treatment of stemness-derived resistant tumor. *Acta Pharm Sin B* 2023;**13**: 1262−73.
259. Choi W, Kohane DS. Hybrid nanoparticle-hydrogel systems for drug delivery depots and other biomedical applications. *ACS Nano* 2024; **18**:22780−92.
260. Zhu Y, Yao ZC, Li S, Ma J, Wei C, Yu D, et al. An mRNA lipid nanoparticle-incorporated nanofiber-hydrogel composite for cancer immunotherapy. *Nat Commun* 2025;**16**:5707.
261. Ghitman J, Biru EI, Stan R, Iovu H. Review of hybrid PLGA nanoparticles: future of smart drug delivery and theranostics medicine. *Mater Des* 2020;**193**:108805.
262. Silva-Pilipich N, Beloki U, Salaberry L, Smerdou C. Self-amplifying RNA: a second revolution of mRNA vaccines against COVID-19. *Vaccines* 2024;**12**:318.
263. Lu RM, Hsu HE, Perez S, Kumari M, Chen GH, Hong MH, et al. Current landscape of mRNA technologies and delivery systems for new modality therapeutics. *J Biomed Sci* 2024;**31**:89.
264. Ong EZ, Yee JX, Ooi JSG, Syenina A, de Alwis R, Chen S, et al. Immune gene expression analysis indicates the potential of a self-amplifying COVID-19 mRNA vaccine. *Npj Vaccines* 2022;**7**:154.
265. De Lombaerde E, Cui X, Chen Y, Zhong Z, Deckers J, Mencarelli G, et al. Amplification of protein expression by self-amplifying mRNA delivered in lipid nanoparticles containing a β-aminoester ionizable lipid correlates with reduced innate immune activation. *ACS Nano* 2024;**18**:28311−24.
266. Kristensen LS, Andersen MS, Stagsted LVW, Ebbesen KK, Hansen TB, Kjems J. The biogenesis, biology and characterization of circular RNAs. *Nat Rev Genet* 2019;**20**:675−91.
267. Liu X, Zhang Y, Zhou SR, Dain LR, Mei L, Zhu GZ. Circular RNA: an emerging frontier in RNA therapeutic targets, RNA therapeutics, and mRNA vaccines. *J Control Release* 2022;**348**:84−94.
268. Jiang W, Xiao D, Wu C, Yang J, Peng X, Chen L, et al. Circular RNA-based therapy provides sustained and robust neuroprotection for retinal ganglion cells. *Mol Ther Nucleic Acids* 2024;**35**:102258.
269. Qu L, Yi Z, Shen Y, Lin L, Chen F, Xu Y, et al. Circular RNA vaccines against SARS-CoV-2 and emerging variants. *Cell* 2022;**185**: 1728−44.e16.
270. Melamed JR, Hajj KA, Chaudhary N, Strelkova D, Arral ML, Pardi N, et al. Lipid nanoparticle chemistry determines how nucleoside base modifications alter mRNA delivery. *J Control Release* 2022;**341**:206−14.
271. Paunovska K, Sago CD, Monaco CM, Hudson WH, Castro MG, Rudoltz TG, et al. A direct comparison of *in vitro* and *in vivo* nucleic acid delivery mediated by hundreds of nanoparticles reveals a weak correlation. *Nano Lett* 2018;**18**:2148−57.
272. Lindsay S, Hussain M, Binici B, Perrie Y. Exploring the challenges of lipid nanoparticle development: the *in vitro-in vivo* correlation gap. *Vaccines* 2025;**13**:339.
273. Lam K, Schreiner P, Leung A, Stainton P, Reid S, Yaworski E, et al. Optimizing lipid nanoparticles for delivery in primates. *Adv Mater* 2023;**35**:e2211420.
274. Zenhausern R, Jang B, Echeverri ES, Gentry K, Calkins R, Curran EH, et al. Lipid nanoparticle screening in nonhuman primates with minimal loss of life. *Nat Biotechnol* 2025. Available from: https://doi.org/10.1038/s41587-025-02711-y.
275. Connors J, Joyner D, Mege NJ, Cusimano GM, Bell MR, Marcy J, et al. Lipid nanoparticles (LNP) induce activation and maturation of antigen presenting cells in young and aged individuals. *Commun Biol* 2023;**6**:188.
276. Hussain M, Ferguson-Ugorenko A, Macfarlane R, Orr N, Clarke S, Wilkinson MJA, et al. Mind the age gap: expanding the age window for mRNA vaccine testing in mice. *Vaccines* 2025;**13**:370.
277. Weinberger B. Adjuvant strategies to improve vaccination of the elderly population. *Curr Opin Pharmacol* 2018;**41**:34−41.
278. Smith OA, Fujimoto B, Wong TAS, To A, Odo T, Ball A, et al. Impact of metabolic states on SARS-CoV-2 vaccine responses in mouse models of obesity and diabetes. *Covid* 2025;**5**:2.
279. Ai L, Li Y, Zhou L, Yao W, Zhang H, Hu Z, et al. Lyophilized mRNA-lipid nanoparticle vaccines with long-term stability and high antigenicity against SARS-CoV-2. *Cell Discov* 2023;**9**:9.

280. Muramatsu H, Lam K, Bajusz C, Laczkó D, Karikó K, Schreiner P, et al. Lyophilization provides long-term stability for a lipid nanoparticle-formulated, nucleoside-modified mRNA vaccine. *Mol Ther* 2022;**30**:1941−51.
281. Lundqvist M, Stigler J, Cedervall T, Berggard T, Flanagan MB, Lynch I, et al. The evolution of the protein corona around nanoparticles: a test study. *ACS Nano* 2011;**5**:7503−9.
282. Sayers EJ, Peel SE, Schantz A, England RM, Beano M, Bates SM, et al. Endocytic profiling of cancer cell models reveals critical factors influencing LNP-mediated mRNA delivery and protein expression. *Mol Ther* 2019;**27**:1950−62.
283. Rybak SL, Murphy RF. Primary cell cultures from murine kidney and heart differ in endosomal pH. *J Cell Physiol* 1998;**176**: 216−22.